

NUMERICAL EXPERIMENTS WITH THE PARTICLE METHOD
FOR THE WIGNER EQUATION
IN HIGH-FREQUENCY PARAXIAL PROPAGATION

E. FERGADAKIS

ABSTRACT. In this work we perform some numerical experiments for the Wigner equation, at relatively high frequencies and for models whose fields develop caustics, by using the particle method and the particle-in-cell technique. The accuracy and the efficiency of the particle method is investigated using either analytical solutions of the Wigner equation or FEM solutions of the associated wave field.

TABLE OF CONTENTS

1. Introduction	3
2. Paraxial approximation	
2.1 Physical conditions	5
2.2 Derivation of the parabolic wave equation	6
2.3 Geometrical acoustics and parabolic approximation	9
2.4 The high-frequency regime	10
3. The Wigner equation	
3.1 The Wigner transform	11
3.2 The Wigner equation for the Schrödinger equation	13
4. The particle method	
4.1 The particle method for the transport equation	18
4.2 The particle method for the Wigner equation	21
5. Numerical examples	
5.1 Example 1: Harmonic oscillator	24
5.1.1 Initial data and potential	24
5.1.2 Integration methods	24
5.1.3 Numerical results	28
5.1.4 Particle in cell (PIC) methods	30
5.1.5 Numerical results for the PIC method	30
5.2 Example 2: Quartic oscillator	32
5.2.1 The convolution term	32
5.2.2 Numerical results for the quartic oscillator	32
References	33

1. INTRODUCTION.

The parabolic wave equation (Schrödinger equation), is a paraxial approximation to the Helmholtz equation, which has applications to many different wave propagation problems arising in science and engineering. It seems to appear for first time in the work of Leontovich and Fock [FO] (see also [Fl], [BB], [BK]) in the mid-1940's, who applied the method to describe the propagation of electromagnetic waves along the surface of the earth. Later, parabolic approximation method was applied to many other fields, like in plasma physics, for the study of beam propagation [TAP2], in seismology for understanding seismic waves in earth's crust, in laser optics ("quasi-optical" equation method), and in the investigation of random waves [TAT1]. Another important field where parabolic approximation has been established as a fundamental tool is underwater acoustics. At the beginning the method was introduced by Tappert [TAP1] for modelling and computing low-frequency, long-range propagation of sound waves in the ocean, but now the method is widely used for computations to much higher frequencies.

The present work is related to the problem of paraxial propagation (Schrödinger equation) in relatively high frequencies (or equivalently, after rescaling, for large Fresnel numbers). Our approach is based on the reformulation (via the Wigner transform) of the initial value problem for the Schrödinger equation as an initial value problem for the (integro-differential) Wigner equation in phase space. The Wigner transform has been introduced since 1932, as an alternative to non-existing joint probability densities in quantum theory [WIG] (see also [TAT2]). It has not received much attention in Applied Mathematics literature, until very recently when Markowich and his collaborators [GM], [GMMP] employed this equation for analyzing semiconductor devices and related wave problems, and Papanicolaou [PR] who used the Wigner transform for investigating waves in random media and rigorously deriving the related radiation transport equations. Concerning classical scattering theory, Perthame and his collaborators [BKP], [RP] applied the Wigner transform to analyze the high frequency Helmholtz equation with a source term. It is however interesting to note that the Wigner distribution (as it is usually referred in Physics and Engineering, especially in signal processing) has been used in heuristic studies of classical waves since seventies. For example, Tappert [TAP2] has used the Wigner distribution for performing diffractive ray tracing of laser beams and he has proposed a "quasiparticle" representation as a tool for the numerical treatment of the problem. An interesting review on the "quasiparticle view" of wave propagation until 1980 has been presented by Marcuvitz [MA]. For later and rigorous mathematical developments, someone should refer to Lions and Paul [LP] and Papanicolaou and Ryzhik [PR].

Very recently, Filippas and Makrakis [FM] have initiated the study of high-frequency asymptotics near caustics, by employing an Airy-type approximation of the Wigner function as an approximate solution of the Wigner equation near the Lagrangian manifold of geometrical optics. In the direction of the numerical solution of the Wigner equation, when the rays of the corresponding geometrical optics' problem (WKB solution) develop caustics, a first attempt has been done by Kalligiannaki [KAL] using the standard method of particles for some simple standard models (harmonic oscillator and potential barrier). In the present work we perform some numerical experiments for the harmonic and quartic oscillators using different formulations for initializing the standard particle method, and also the so-called particle-in-cell technique for reducing the computational load.

The contents of the work are as follows. In Section 2 we present the basics of the parabolic equation. In Section 3 we introduce the Wigner transform and its basic properties, and we derive the Wigner equation for the Schrödinger equation. In Section 4 we present the particle method for the transport and the Wigner equation. Finally, in Section 5 we perform numerical experiments with the particle and the particle in cell methods for the harmonic and the quartic oscillator. The numerical results of the particle method are well compared with a FEM solution for intermediate frequencies. For very high frequencies the FEM solution seems to be inaccurate and it cannot be

improved, and on the other hand, the particle solution needs a tremendous big number of particles in order to be in reasonable agreement with the available analytical solution for the harmonic oscillator. A similar situation appears in the case of the quartic oscillator for which an analytical solution is not available.

2. PARAXIAL APPROXIMATION.

2.1 Physical conditions.

The parabolic approximation method (more precisely, paraxial approximation), as is applied to the long-range propagation of acoustic signals in the ocean, is based on the special propagation features of sound channel mode of propagation (guided waves), which makes possible this phenomenon. Sound channel propagation takes place in a waveguide that is relatively thin in the vertical direction, and greatly elongated horizontally, and which confines the acoustic waves within the water column and prevents their interaction with the bottom.

Comparing the approximation under discussion with the other two basic approximating methods in underwater acoustics, that is geometrical acoustics and normal-mode expansions, we can observe its advantages. Geometrical acoustics methods need small wavelengths in order to have negligible diffraction effects, and separation of variables methods are valid only in an exactly horizontally stratified ocean. Though, parabolic approximation methods retain diffraction effects and are valid for more realistic oceans, where horizontal variation of the refraction index is allowed.

The fact that the largest angles of interest in long range propagation are rather small sets the stage of the parabolic approximation. In order to explain why long range propagation corresponds essentially to small angles of propagation, we use the geometrical acoustics for a horizontally stratified ocean, and we assume that all bottom interacting rays are attenuated rapidly enough, so that they don't contribute to long range propagation. Indeed, by Snell's law, the maximum angle of propagation, with respect to the horizontal direction, is given by

$$(2.1.1) \quad \theta_l = \cos^{-1} \left(\frac{c_{min}}{c_{max}} \right) ,$$

where c_{min} , c_{max} are the extreme values of the sound speed in the ocean. For the derivation of (2.1.1) we consider the Hamiltonian

$$H(x, z, k_x, k_z) = \frac{1}{2}(\mathbf{k}^2 - \eta^2(z)) , \quad k^2 = k_x^2 + k_z^2 ,$$

corresponding to the Helmholtz equation with refraction index $\eta(z)$. The rays (characteristics) emanating from $x = z = 0$, are found from the corresponding Hamiltonian system

$$(2.1.2) \quad \begin{cases} \frac{dx}{dt} = k_x, & \frac{dz}{dt} = k_z \\ \frac{dk_x}{dt} = 0, & \frac{dk_z}{dt} = (\eta^2(z)/2)' \\ x(0) = 0, & z(0) = 0 \\ k_x(0) = k_{x_0}, & k_z(0) = k_{z_0} . \end{cases}$$

Solving this system we obtain

$$k_z^2 = k_{z_0}^2 - \eta^2(0) + \eta^2(z) ,$$

and

$$\left(\frac{dz}{dx} \right)^2 = \frac{k_z^2}{k_{x_0}^2} .$$

At the bottom depth $z = z_b$, we want $k_z|_{z=z_b} = 0$, and noting that $\frac{dz}{dx} = \sin\theta$, $\theta_b = 0$ we have

$$\cos\theta_l = (1 - \sin^2\theta_l)^{1/2} = \left(1 - \left(\frac{k_{z_0}}{\mathbf{k}^2(0)} \right)^2 \right)^{1/2} = \frac{\eta(z_b)}{\eta(0)} = \frac{\frac{c_0}{c_{max}}}{\frac{c_0}{c_{min}}}$$

which gives us (2.1.1).

Moreover, if we put $\Delta c = c_{max} - c_{min}$, where c_0 is an average sound speed, then

$$\frac{c_{min}}{c_{max}} = 1 - \frac{\Delta c}{c_{max}},$$

and using

$$\cos(\theta_l) \approx 1 - \frac{\theta_l^2}{2}$$

for small θ_l , we find

$$\theta_l \approx \frac{2\Delta c}{c_{max}} \approx \frac{2\Delta c}{c_0}$$

Typically, in the ocean $c_0 \approx 1500m/sec$ and $\Delta c/c_0 \lesssim 0.04$, and therefore $\theta_l \lesssim 16^\circ$. This is the reason that sometimes the parabolic equation we will derive in the sequel is called the 16° -approximation in physics and engineering literature.

2.2 Derivation of the parabolic wave equation.

We proceed now to the derivation of the parabolic wave equation for realistic ocean environments, which even though they may not be analytically solvable, are especially well adapted for numerical computations.

We consider a fixed point source at $x = y = 0$, $z = z_s$ which radiates a spherical wave at fixed frequency ω , and we assume that the refraction index of the ocean depends on all three spatial coordinates, but not on time. We also assume that the density of the fluid is constant, and that the volume attenuation is zero.

Then, the complex acoustic pressure satisfies the Helmholtz equation, which in cylindrical coordinates (r, ϕ, z) is written in the form

$$(2.2.1) \quad \Delta p + k_0^2 \eta^2(z, r, \phi) p = -\delta(\vec{x}),$$

where

$$\Delta p = \frac{1}{r} \frac{\partial}{\partial r} \left(r \frac{\partial p}{\partial r} \right) + \frac{\partial^2 p}{\partial z^2} + \frac{1}{r^2} \frac{\partial^2 p}{\partial \phi^2}$$

is the Laplacian, and

$$\delta(\vec{x}) = \frac{1}{2\pi r} \delta(z - z_s) \delta(r),$$

is the Dirac function in cylindrical coordinates. Here $k_0 = \frac{\omega}{c_0}$, is the wavenumber, ω is the angular acoustic frequency and $\eta(z, r, \phi) = c_0/c(z, r, \phi)$ is the refraction index, both corresponding to a reference sound speed c_0 .

For solving equation (2.2.1) we must determine the boundary conditions on the surface $z = 0$ and the bottom of the ocean. As surface boundary condition is traditionally used the pressure release condition $p(z = 0, r, \phi) = 0$. The bottom boundary condition depends on the modeling of the bottom. Generally waves that penetrate deep into the subbottom layers do not contribute significantly to long range propagation and should be removed from the calculation. This effect is sometimes modeled by complexifying the refraction index as $\eta^2(z, r, \phi) + iv(z, r, \phi)$, where v increase rapidly for z much greater than the depth of the ocean and then cutting off the calculational domain at a depth where the acoustic field has been reduced to a negligible amplitude. However, such a modeling is not always consistent with the underlying continuum mechanics, and rigorous

boundary conditions assuming fluid, elastic or poroelastic bottoms can be devised in the expense of complication of the numerical treatment of the problem.

Moreover, radiation conditions of Sommerfeld type must be prescribed for $r \rightarrow \infty$ to guarantee uniqueness of the solution of the Helmholtz equation (cf. [GX], [XU]) and they will be built in the asymptotic decomposition of the pressure field below (cf. eq. (2.2.2)).

For the case that we are assuming that all significant acoustic waves are propagating mostly in the horizontal direction away from the source, the acoustic field may be represented as

$$(2.2.2) \quad p(z, r, \phi) = \psi(z, r, \phi) H_0^{(1)}(k_0 r)$$

where $H_0^{(1)}(k_0 r)$ is the Hankel function of zero order and first kind (outgoing radial solution of the Helmholtz equation in cylindrical coordinates), and ψ is an envelope function that depends on depth, range and azimuth. The above representation is expected to be a good approximation only when $k_0 r \gg 1$. For low frequencies this conditions holds in the far field of the point source, but for higher frequencies the range of validity may be reduced. Also, since the representation (2.2.2) is not expected to hold near the source, the source term at equation (2.2.1) will be omitted, and we will consider the homogeneous Helmholtz equation

$$(2.2.3) \quad \Delta p + k_0^2 \eta^2(z, r, \phi) p(z, r, \phi) = 0 .$$

In order to derive an equation for the envelope ψ we substitute (2.2.2) into (2.2.3). First we compute

$$\begin{aligned} \Delta(\psi H_0^{(1)}(k_0 r)) &= \\ &= \frac{\partial^2 \psi}{\partial r^2} H_0^{(1)}(k_0 r) + \left(\frac{2 \partial(H_0^{(1)}(k_0 r))}{\partial r} + \frac{1}{r} H_0^{(1)}(k_0 r) \right) \frac{\partial \psi}{\partial r} + \\ &+ \frac{\partial^2 \psi}{\partial z^2} H_0^{(1)}(k_0 r) + \frac{1}{r^2} \frac{\partial^2 \psi}{\partial \phi^2} H_0^{(1)}(k_0 r) + \frac{1}{r} \frac{\partial(H_0^{(1)}(k_0 r))}{\partial r} \psi + \frac{\partial^2}{\partial r^2} (H_0^{(1)}(k_0 r)) \psi . \end{aligned}$$

Then, we have

$$\begin{aligned} &\left(\Delta(\psi H_0^{(1)}(k_0 r)) + k_0^2 \eta^2(\psi H_0^{(1)}(k_0 r)) \right) \frac{1}{H_0^{(1)}(k_0 r)} = \\ &= \frac{\partial^2 \psi}{\partial r^2} + \left(\frac{2}{H_0^{(1)}(k_0 r)} \frac{\partial H_0^{(1)}(k_0 r)}{\partial r} + \frac{1}{r} \right) \frac{\partial \psi}{\partial r} + \frac{\partial^2 \psi}{\partial z^2} + \frac{1}{r^2} \frac{\partial^2 \psi}{\partial \phi^2} + \\ &+ \left(\frac{1}{r} \frac{1}{H_0^{(1)}(k_0 r)} \frac{\partial H_0^{(1)}(k_0 r)}{\partial r} + \frac{1}{H_0^{(1)}(k_0 r)} \frac{\partial^2 H_0^{(1)}(k_0 r)}{\partial r^2} \right) \psi + k_0^2 \eta^2 \psi = 0 , \end{aligned}$$

which gives

$$(2.2.4) \quad \frac{\partial^2 \psi}{\partial r^2} + \left(\frac{2}{H_0^{(1)}(k_0 r)} \frac{\partial H_0^{(1)}(k_0 r)}{\partial r} + \frac{1}{r} \right) \frac{\partial \psi}{\partial r} + \frac{\partial^2 \psi}{\partial z^2} + \frac{1}{r^2} \frac{\partial^2 \psi}{\partial \phi^2} + k_0^2 (\eta^2 - 1) \psi = 0 .$$

Now, for $k_0 r \gg 1$, by the asymptotics of the Hankel function we have

$$H_0^{(1)}(k_0 r) \sim \left(\frac{2}{i\pi k_0 r} \right)^{1/2} e^{ik_0 r} ,$$

and

$$\frac{\partial H_0^{(1)}(k_0 r)}{\partial r} = \left(\frac{2}{i\pi k_0 r} \right)^{1/2} e^{ik_0 r} \left(-\frac{1}{2r} + ik_0 \right),$$

and thus

$$\frac{2}{H_0^{(1)}(k_0 r)} \frac{\partial H_0^{(1)}(k_0 r)}{\partial r} + \frac{1}{r} = 2ik_0 \left(1 + O\left(\frac{1}{k_0^2 r^2}\right) \right).$$

Consequently neglecting the terms of order $1/k_0^2 r^2$, equation (2.2.4) reduces to

$$(2.2.5) \quad \frac{\partial^2 \psi}{\partial r^2} + 2ik_0 \frac{\partial \psi}{\partial r} + \frac{\partial^2 \psi}{\partial z^2} + \frac{1}{r^2} \frac{\partial^2 \psi}{\partial \phi^2} + k_0^2 (\eta^2 - 1) \psi = 0.$$

If the main radial dependence of the acoustic field is $e^{ik_0 r}$ for some k_0 , then the envelope function ψ will vary slowly as a function of r in the wavelength scale, that is

$$\frac{\partial \psi}{\partial r} \ll k_0 \psi,$$

and therefore we can neglect the term $\frac{\partial^2 \psi}{\partial r^2}$ in (2.2.5) with a small error. This leads to the desired approximation, and the parabolic wave equation reads as follows

$$(2.2.6) \quad 2ik_0 \frac{\partial \psi}{\partial r} + \frac{\partial^2 \psi}{\partial z^2} + \frac{1}{r^2} \frac{\partial^2 \psi}{\partial \phi^2} + k_0^2 (\eta^2 - 1) \psi = 0.$$

In the case that the variation of the ocean in azimuth is very gradual, we may omit the scattering in the horizontal azimuthal direction, that is to neglect the term $\partial^2 \psi / \partial \phi^2$ in (2.2.6), which means that we consider $\psi = \psi(r, z)$.

Then the parabolic equation becomes

$$(2.2.7) \quad i \frac{\partial \psi(z, r)}{\partial r} + \frac{1}{2k_0} \frac{\partial^2}{\partial z^2} \psi(z, r) + \frac{k_0}{2} (\eta^2(z, r) - 1) \psi(z, r) = 0.$$

The last equation has the form of the standard Schrödinger equation

$$(2.2.8) \quad i\epsilon \partial_t \psi_\epsilon = -\frac{\epsilon^2}{2} \partial_z^2 \psi_\epsilon + V(z, t) \psi_\epsilon(z, t),$$

with the correspondence

$$(2.2.9) \quad \epsilon = 1/k_0, \quad t = r, \quad V(z, t) = (1 - \eta^2)/2,$$

that is, the range r plays the role of time, and the potential may depend both on space z and time t , which makes the problem quite different from the corresponding quantum mechanical scattering equation.

Equation (2.2.7) is the most widely used parabolic wave equation in underwater acoustics. Other approximations like wide-angle parabolic equation have been devised, which are capable of greater propagation angles. In general, a whole hierarchy of paraxial equations can be derived by certain asymptotic approximations of the symbol of the pseudodifferential operator arising in one-way factorization of the Helmholtz equation (cf. [TAP1], [LEE]).

The initial data for equation (2.2.7) are modeled on the basis of a near source expansion of the solution of the Helmholtz equation (2.2.1), see, e.g., [COL]. However, a systematic asymptotic derivation of the initial conditions for (2.2.7) is still lacking.

2.3 Geometrical acoustics and parabolic approximation.

Observing that equation (2.2.7) is a wave-type equation, we can perform a geometrical acoustics approximation. Therefore, in order to ensure the validity of the parabolic approximation we shall compare the geometrical acoustics approximation [BLP], [KO1], [KO2] of the parabolic wave equation and that of the Helmholtz equation.

We assume that the ocean is horizontally stratified. Then, the index of refraction depends only on depth, i.e. $\eta = \eta(z)$. We also assume that the acoustic frequency is high enough so that we can perform the geometrical acoustics approximation. The Hamiltonian for the Helmholtz equation is given by

$$H(z, r, k_z, k_r) = \frac{1}{2}(\mathbf{k}^2 - \eta^2(z)) , \quad \mathbf{k} = (k_z, k_r) ,$$

and the exact ray equations are given by the corresponding Hamiltonian system

$$\begin{aligned} \frac{dr}{dt} &= k_r, & \frac{dk_r}{dt} &= 0 \\ \frac{dz}{dt} &= k_z, & \frac{dk_z}{dt} &= (\eta^2(z)/2)' . \end{aligned}$$

From this system it follows $k_r = \text{constant}$, and

$$(2.3.1) \quad \frac{d^2 z}{dr^2} = \frac{1}{s^2} \frac{d}{dz} \left(\frac{1}{2} \eta^2(z) \right) ,$$

where $s := \eta(z) \cos \theta = \text{constant}$ is Snell's invariant. The angle θ between the rays and the horizontal direction r is given by $\tan \theta = k_z/k_r$.

In order to derive the corresponding rays for the parabolic wave equation (2.2.7), we ask for solutions $\psi(z, r)$ in the form

$$\psi(z, r) = A(z, r) e^{i\Phi(z, r)} .$$

Substituting this ansatz into the parabolic wave equation (2.2.7), we have

$$\begin{aligned} & i \left(\frac{\partial A(z, r)}{\partial r} + i A(z, r) \frac{\partial \Phi(z, r)}{\partial r} \right) + \\ & + \frac{1}{2k_0} \left(\frac{\partial^2 A(z, r)}{\partial z^2} + 2i \frac{\partial A(z, r)}{\partial z} \frac{\partial \Phi(z, r)}{\partial z} + i A(z, r) \frac{\partial^2 \Phi(z, r)}{\partial z^2} - A(z, r) \left(\frac{\partial \Phi(z, r)}{\partial z} \right)^2 \right) + \\ & + \frac{k_0}{2} (\eta^2(z) - 1) A(z, r) = 0 . \end{aligned}$$

Equating the real and imaginary parts of the last equation to zero, we obtain the system

$$(2.3.2) \quad \frac{\partial A(z, r)}{\partial r} + \frac{1}{k_0} \frac{\partial A(z, r)}{\partial z} \frac{\partial \Phi(z, r)}{\partial z} + \frac{1}{2k_0} A(z, r) \frac{\partial^2 \Phi(z, r)}{\partial z^2} = 0 ,$$

$$(2.3.3) \quad A(z, r) \frac{\partial \Phi(z, r)}{\partial r} + \frac{1}{2k_0} \frac{\partial^2 A(z, r)}{\partial z^2} - \frac{1}{2k_0} \left(\frac{\partial \Phi(z, r)}{\partial z} \right)^2 A(z, r) + \frac{k_0}{2} (\eta^2(z) - 1) A(z, r) = 0 .$$

Setting

$$\theta(z, r) = \frac{1}{k_0} \frac{\partial \Phi(z, r)}{\partial z} ,$$

the equations (2.3.2) and (2.3.3) are written in the form

$$(2.3.4) \quad \frac{\partial A^2(z, r)}{\partial r} + \frac{\partial}{\partial z} (\theta(z, r) A^2(z, r)) = 0 ,$$

and

$$(2.3.5) \quad \frac{\partial \theta(z, r)}{\partial r} + \theta(z, r) \frac{\partial \theta(z, r)}{\partial z} = \frac{1}{2k_0^2} \frac{\partial}{\partial z} \left(\frac{1}{A(z, r)} \frac{\partial^2 A(z, r)}{\partial z^2} \right) + \frac{\partial}{\partial z} \left(\frac{1}{2} \eta^2(z) \right) ,$$

respectively.

In performing the geometrical acoustics approximation, we take the formal limit $k_0 \rightarrow \infty$ of (2.3.5), which is approximated by

$$(2.3.6) \quad \frac{\partial \theta(z, r)}{\partial r} + \theta(z, r) \frac{\partial \theta(z, r)}{\partial z} = \frac{\partial}{\partial z} \left(\frac{1}{2} \eta^2(z) \right) .$$

Moreover, from (2.3.4) we see that the acoustic power $A^2(z, r)$ is invariantly transported along the characteristic curves

$$(2.3.7) \quad \frac{dz}{dr} = \theta(z, r) .$$

Combining (2.3.6) and (2.3.7), we find the following equation for the rays of the parabolic wave equation

$$(2.3.8) \quad \frac{d\theta(z, r)}{dr} = \frac{d}{dz} \left(\frac{1}{2} \eta^2(z) \right) .$$

Comparing the ray equations (2.3.1) and (2.3.8), we note that ray equations for the parabolic wave equation are the same as those for the Helmholtz equation with $s = 1$. But in order that $s \sim 1$ we need that $\eta(z) \approx 1$ and $\theta \ll 1$. This conclusion verifies that small angles of propagation is a necessary condition for the parabolic approximation to be valid.

2.4. The high-frequency regime.

The parabolic equation (2.2.7) has been traditionally used for small frequencies on the basis of a physical argument saying that the volume absorption of sound energy increases very fast with frequency. More recently computations based on the parabolic equation have been used for higher frequencies, in a somehow inconsistent way, but the numerical results seem to be reasonable. On the other hand, the Helmholtz equation (2.2.1) and its approximation (2.2.7) are derived from first principles of mechanics with no dissipation in the basic equations. Dissipation is usually introduced a posteriori by complexifying the frequency, and this corresponds to a particular energy dissipation mechanism that may be not compatible with the underlying continuum mechanics.

Assuming here that there is not any dissipation, we investigate the high frequency case (ϵ small), thus attempting to reduce the range of validity of the numerical computation, and to perform as much as possible "near field" calculations, as the actual parameter entering the derivation of (2.2.7) is $k_0 r$. Moreover, by rescaling the equation (2.2.7) it is always possible to introduce in place of $\epsilon = 1/k_0$, the parameter $\epsilon = 1/F$, $F = k_0 Z^2/R$ being the Fresnel number, with R, Z the characteristic horizontal and vertical distances of the wave field.

3.The Wigner equation.

3.1 The Wigner transform. [PR],[LP]

For any smooth function $\psi(\mathbf{x})$ rapidly decaying at infinity, that is $\psi \in \mathcal{S}(\mathbb{R})$, the Wigner transform of ψ is a quadratic transform defined by

$$(3.1.1) \quad W[\psi](x, k) = W(x, k) = \frac{1}{2\pi} \int_{\mathbb{R}} e^{-iky} \psi(x + \frac{y}{2}) \overline{\psi}(x - \frac{y}{2}) dy$$

where $\overline{\psi}$ is the complex conjugate of ψ . The Wigner transform is a defined in phase space \mathbb{R}_{xk} , it is real, and it has many important properties, the most remarkable of them being the following.

First, the k -integral of $W(x, k)$ is the energy density of ψ

$$(3.1.2) \quad \int_{\mathbb{R}} W(x, k) dk = |\psi(x)|^2 .$$

In fact, we have

$$\begin{aligned} \int_{\mathbb{R}} W(x, k) dk &= \frac{1}{2\pi} \int_{\mathbb{R}} \int_{\mathbb{R}} e^{-iky} \psi(x + \frac{y}{2}) \overline{\psi}(x - \frac{y}{2}) dy dk = \\ &= \int_{\mathbb{R}} \left(\frac{1}{2\pi} \int_{\mathbb{R}} e^{-iky} dk \right) \psi(x + \frac{y}{2}) \overline{\psi}(x - \frac{y}{2}) dy = \\ &= \int_{\mathbb{R}} \delta(y) \psi(x + \frac{y}{2}) \overline{\psi}(x - \frac{y}{2}) dy = \psi(x) \overline{\psi}(x) = |\psi(x)|^2 . \end{aligned}$$

Here δ is the δ -function, and we used the Fourier transform $\delta(y) = \frac{1}{2\pi} \int_{\mathbb{R}} e^{-iky} dk$.

Second, the first moment in k of $W(x, k)$ is the energy flux

$$(3.1.3) \quad \int_{\mathbb{R}} kW(x, k) dk = \frac{1}{2i} (\psi(x) \overline{\psi}'(x) - \overline{\psi}(x) \psi'(x)) = \mathcal{F}(x) .$$

In fact, we have

$$\begin{aligned} \int_{\mathbb{R}} kW(x, k) dk &= \int_{\mathbb{R}} \left(\frac{1}{2\pi} \int_{\mathbb{R}} ke^{-iky} dk \right) \psi(x + \frac{y}{2}) \overline{\psi}(x - \frac{y}{2}) dy = -\frac{1}{i} \int_{\mathbb{R}} \delta'(y) \psi(x + \frac{y}{2}) \overline{\psi}(x - \frac{y}{2}) dy = \\ &= \frac{1}{i} \int_{\mathbb{R}} \delta(y) \left(\frac{1}{2} \psi'(x + \frac{y}{2}) \overline{\psi}(x - \frac{y}{2}) - \frac{1}{2} \overline{\psi}'(x - \frac{y}{2}) \psi(x + \frac{y}{2}) \right) dy = \\ &= \frac{1}{2i} \left(\overline{\psi}(x) \psi'(x) - \psi(x) \overline{\psi}'(x) \right) . \end{aligned}$$

The x to k duality in phase space can be recognized using the alternative definition

$$(3.1.4) \quad W(x, k) = \int_{\mathbb{R}} e^{ipx} \widehat{\psi}(-k - \frac{p}{2}) \overline{\widehat{\psi}(-k + \frac{p}{2})} dp ,$$

where $\widehat{\psi}(k) = \frac{1}{2\pi} \int_{\mathbb{R}} e^{ikz} \psi(z) dz$ denotes the Fourier transform of ψ .

In fact, the definitions (3.1) and (3.2) are equivalent, since we have

$$\begin{aligned}
W(x, k) &= \frac{1}{2\pi} \int_{\mathbb{R}} e^{-iky} \psi(x + \frac{y}{2}) \overline{\psi}(x - \frac{y}{2}) dy = \frac{1}{2\pi} \int_{\mathbb{R}} e^{-iky} \int_{\mathbb{R}} e^{-iz(x+\frac{y}{2})} \widehat{\psi}(z) dz \int_{\mathbb{R}} \overline{e^{-iw(x-\frac{y}{2})} \widehat{\psi}(w)} dw dy = \\
&= \frac{1}{2\pi} \int_{\mathbb{R}} e^{-iky} \int_{\mathbb{R}} e^{-iz(x+\frac{y}{2})} \widehat{\psi}(z) dz \int_{\mathbb{R}} e^{iw(x-\frac{y}{2})} \overline{\widehat{\psi}(w)} dw dy = \\
&= \int_{\mathbb{R}} \int_{\mathbb{R}} \left(\frac{1}{2\pi} \int_{\mathbb{R}} e^{-iy(k+\frac{z}{2}+\frac{w}{2})} dy \right) e^{-i(z-w)x} \widehat{\psi}(z) \overline{\widehat{\psi}(w)} dz dw = \\
&= \int_{\mathbb{R}} \int_{\mathbb{R}} \delta(k + \frac{z}{2} + \frac{w}{2}) e^{-i(z-w)x} \widehat{\psi}(z) \overline{\widehat{\psi}(w)} dz dw = \\
&= 2 \int_{\mathbb{R}} e^{-i2(k+z)x} \widehat{\psi}(z) \overline{\widehat{\psi}(-2k-z)} dz = \int_{\mathbb{R}} e^{ipx} \widehat{\psi}(-k - \frac{p}{2}) \overline{\widehat{\psi}(-k + \frac{p}{2})} dp = \\
&= \int_{\mathbb{R}} e^{ipx} \widehat{\psi}(-k - \frac{p}{2}) \overline{\widehat{\psi}(-k + \frac{p}{2})} dp .
\end{aligned}$$

In the case of high frequency wave propagation, the WKB method suggests solutions of the form

$$\psi^\epsilon(x, t) = e^{iS(x,t)/\epsilon} A(x, t) , \quad \epsilon \rightarrow 0 ,$$

where S is a real-valued and smooth phase, and A is a real-valued smooth amplitude of compact support. The Wigner distribution of $\psi^\epsilon(x)$ is

$$W(x, k) = \frac{1}{2\pi} \int_{\mathbb{R}} e^{-iky} e^{iS(x+\frac{y}{2})/\epsilon} A(x + \frac{y}{2}) e^{-iS(x-\frac{y}{2})/\epsilon} \overline{A}(x - \frac{y}{2}) dy ,$$

but $W(x, k)$ does not converge as $\epsilon \rightarrow 0$. However, it can be shown that the rescaled version of $W(x, k)$,

$$W^\epsilon(x, k) = \frac{1}{\epsilon} W(x, \frac{k}{\epsilon})$$

converges weakly as $\epsilon \rightarrow 0$ [PR], [LP].

Indeed, proceeding formally, we rewrite W^ϵ in the form

$$W^\epsilon(x, k) = \frac{1}{2\pi} \int_{\mathbb{R}} e^{-iky} A(x + \frac{\epsilon y}{2}) \overline{A}(x - \frac{\epsilon y}{2}) e^{\frac{i}{\epsilon} [S(x+\frac{\epsilon y}{2}) - S(x-\frac{\epsilon y}{2})]} dy ,$$

and we expand in Taylor series about $y = 0$ both A and S . Then, we have

$$\begin{aligned}
A(x + \frac{\epsilon y}{2}) \overline{A}(x - \frac{\epsilon y}{2}) &= \left(A(x) + \frac{\epsilon}{2} y A'(x) + \dots \right) \left(\overline{A}(x) - \frac{\epsilon}{2} y \overline{A}'(x) + \dots \right) \\
&= A(x) \overline{A}(x) + O(\epsilon) = |A(x)|^2 + O(\epsilon) ,
\end{aligned}$$

and

$$\begin{aligned}
S(x + \frac{\epsilon y}{2}) - S(x - \frac{\epsilon y}{2}) &= \left(S(x) + \frac{\epsilon}{2} y S'(x) + \frac{\epsilon^2}{4} S''(x) + \dots \right) - \left(S(x) - \frac{\epsilon}{2} y S'(x) + \frac{\epsilon^2}{4} S''(x) - \dots \right) = \\
&= \epsilon y S'(x) + O(\epsilon^3) .
\end{aligned}$$

Retaining only terms of order $O(1)$ in A and $O(y)$ in S , and integrating the expansion termwise we obtain that $W^\epsilon(x, k)$ "converges" to

$$(3.1.5) \quad W(x, k) = |A(x)|^2 \frac{1}{2\pi} \int_{\mathbb{R}} e^{-i(k-S'(x))y} dy = |A(x)|^2 \delta(k - S'(x)) ,$$

which is a Dirac measure, concentrated on the Lagrangian manifold $k = S'(x)$, associated with the phase of the WKB solution ψ^ϵ [ARN1],[ARN2], and it is the correct weak limit [LP]. More precisely, if Q is any test function in $\mathcal{S}(\mathbb{R}^2)$, then

$$\int_{\mathbb{R}} \int_{\mathbb{R}} Q(x, k) W^\epsilon(x, k) dx dk \rightarrow \int_{\mathbb{R}} Q(x, S'(x)) |A(x)|^2 dx .$$

The above observations suggest that the scaled Wigner transform

$$(3.1.6) \quad \begin{aligned} W^\epsilon(x, k) &= \frac{1}{\epsilon} W(x, \frac{k}{\epsilon}) = \\ &= \frac{1}{2\pi} \int_{\mathbb{R}} e^{-iky} \psi^\epsilon(x + \frac{\epsilon y}{2}) \overline{\psi^\epsilon}(x - \frac{\epsilon y}{2}) dy , \end{aligned}$$

is the correct phase-space object for analyzing high frequency waves.

3.2 The Wigner equation for the Schrödinger equation.

We consider the following initial-value problem for the Schrödinger equation (cf. eq. (2.2.8)), with time-independent potential (this corresponds to range-independent ocean sound speed)

$$(3.2.1) \quad \begin{cases} i\epsilon \partial_t \psi^\epsilon(x, t) = -\frac{\epsilon^2}{2} \partial_x^2 \psi^\epsilon(x, t) + V(x) \psi^\epsilon(x, t) \\ \psi^\epsilon(x, 0) = \psi_0^\epsilon(x, t) . \end{cases}$$

Let $W^\epsilon(x, k, t)$ be the scaled Wigner distribution of $\psi^\epsilon(x, t)$. In order to find the equation that $W^\epsilon(x, k, t)$ satisfies, we start with the identity

$$(3.2.2) \quad \begin{aligned} & i\epsilon \left(\partial_t \psi^\epsilon(x + \frac{\epsilon}{2}y, t) \overline{\phi^\epsilon}(x - \frac{\epsilon}{2}y, t) + \partial_t \overline{\phi^\epsilon}(x - \frac{\epsilon}{2}y, t) \psi^\epsilon(x + \frac{\epsilon}{2}y, t) \right) = \\ & = -\frac{\epsilon^2}{2} \left(\overline{\phi^\epsilon}(x - \frac{\epsilon}{2}y, t) \partial_x^2 \psi^\epsilon(x + \frac{\epsilon}{2}y, t) - \psi^\epsilon(x + \frac{\epsilon}{2}y, t) \partial_x^2 \overline{\phi^\epsilon}(x - \frac{\epsilon}{2}y, t) \right) + \\ & + \left(V(x + \frac{\epsilon}{2}y) - V(x - \frac{\epsilon}{2}y) \right) \psi^\epsilon(x + \frac{\epsilon}{2}y, t) \overline{\phi^\epsilon}(x - \frac{\epsilon}{2}y, t) . \end{aligned}$$

If we put

$$v^\epsilon(x, y, t) = \psi^\epsilon(x + \frac{\epsilon}{2}y, t) \overline{\phi^\epsilon}(x - \frac{\epsilon}{2}y, t)$$

then, we have

$$\partial_x v^\epsilon = \partial_x \psi^\epsilon(x + \frac{\epsilon}{2}y, t) \overline{\phi^\epsilon}(x - \frac{\epsilon}{2}y, t) + \psi^\epsilon(x + \frac{\epsilon}{2}y, t) \partial_x \overline{\phi^\epsilon}(x - \frac{\epsilon}{2}y, t) ,$$

and

$$\begin{aligned} \partial_y \partial_x v^\epsilon &= \frac{\epsilon}{2} \partial_x^2 \psi^\epsilon(x + \frac{\epsilon}{2}y, t) \overline{\phi^\epsilon}(x - \frac{\epsilon}{2}y, t) - \frac{\epsilon}{2} \partial_x \psi^\epsilon(x + \frac{\epsilon}{2}y, t) \partial_x \overline{\phi^\epsilon}(x - \frac{\epsilon}{2}y, t) \\ &+ \frac{\epsilon}{2} \partial_x \psi^\epsilon(x + \frac{\epsilon}{2}y, t) \partial_x \overline{\phi^\epsilon}(x - \frac{\epsilon}{2}y, t) - \frac{\epsilon}{2} \psi^\epsilon(x + \frac{\epsilon}{2}y, t) \partial_x^2 \overline{\phi^\epsilon}(x - \frac{\epsilon}{2}y, t) \\ &= \frac{\epsilon}{2} \left(\partial_x^2 \psi^\epsilon(x + \frac{\epsilon}{2}y, t) \overline{\phi^\epsilon}(x - \frac{\epsilon}{2}y, t) - \psi^\epsilon(x + \frac{\epsilon}{2}y, t) \partial_x^2 \overline{\phi^\epsilon}(x - \frac{\epsilon}{2}y, t) \right) . \end{aligned}$$

Using the above two relations we rewrite (3.2.2) in terms of v^ϵ as follows

$$\begin{aligned} i\epsilon\partial_t v^\epsilon &= -\frac{\epsilon^2}{2}\frac{2}{\epsilon}\partial_y\partial_x v^\epsilon + \left(V(x + \frac{\epsilon}{2}y) - V(x - \frac{\epsilon}{2}y)\right) v^\epsilon \\ &= -\epsilon\partial_y\partial_x v^\epsilon + \left(V(x + \frac{\epsilon}{2}y) - V(x - \frac{\epsilon}{2}y)\right) v^\epsilon . \end{aligned}$$

Multiplying the last equation by $e^{-iky}/2\pi$, and integrating with respect to y we get

$$\begin{aligned} i\epsilon\partial_t \left\{ \frac{1}{2\pi} \int_{\mathbb{R}} e^{-iky} v^\epsilon(x, y, t) dy \right\} &= -\epsilon\partial_x \left\{ \frac{1}{2\pi} \int_{\mathbb{R}} e^{-iky} \partial_y v^\epsilon(x, y, t) dy \right\} \\ &\quad + \frac{1}{2\pi} \int_{\mathbb{R}} e^{-iky} \left(V(x + \frac{\epsilon}{2}y) - V(x - \frac{\epsilon}{2}y) \right) v^\epsilon(x, y, t) dy . \end{aligned}$$

By noting that

$$W^\epsilon(x, k, t) = \frac{1}{2\pi} \int_{\mathbb{R}} e^{-iky} v^\epsilon(x, y, t) dy ,$$

the above equation is written in the form

$$\begin{aligned} i\epsilon\partial_t W^\epsilon(x, k, t) &= -\epsilon\frac{\partial}{\partial x} \left\{ \frac{1}{2\pi} [e^{-iky} v^\epsilon]_{-\infty}^{+\infty} + (ik)\frac{1}{2\pi} \int_{\mathbb{R}} e^{-iky} v^\epsilon(x, y, t) dy \right\} + \\ &\quad \frac{1}{2\pi} \int_{\mathbb{R}} e^{-iky} \left(V(x + \frac{\epsilon}{2}y) - V(x - \frac{\epsilon}{2}y) \right) v^\epsilon(x, y, t) dy . \end{aligned}$$

Assuming now that $\psi^\epsilon(x, t)$ decays fast enough as $|x| \rightarrow \infty$, we have

$$\lim_{|y| \rightarrow +\infty} (e^{-iky} v^\epsilon) = 0 ,$$

and therefore W^ϵ satisfies the equation

$$(3.2.3) \quad \partial_t W^\epsilon(x, k, t) = -k\partial_x W^\epsilon(x, k, t) + I ,$$

where

$$I(x, k, t) = \frac{1}{i\epsilon} \frac{1}{2\pi} \int_{\mathbb{R}} e^{-iky} \left(V(x + \frac{\epsilon}{2}y) - V(x - \frac{\epsilon}{2}y) \right) v^\epsilon(x, y, t) dy .$$

Since $W^\epsilon(x, k, t)$ is the Fourier transform of $v^\epsilon(x, y, t)$, we have

$$v^\epsilon(x, y, t) = \int_{\mathbb{R}} e^{i\xi y} W^\epsilon(x, \xi, t) d\xi ,$$

and we write I as follows

$$\begin{aligned} I &= \frac{1}{i\epsilon} \frac{1}{2\pi} \int_{\mathbb{R}} \int_{\mathbb{R}} e^{-iky} e^{i\xi y} W^\epsilon(x, \xi, t) \left(V(x + \frac{\epsilon}{2}y) - V(x - \frac{\epsilon}{2}y) \right) d\xi dy = \\ &= \frac{1}{i\epsilon} \frac{1}{2\pi} \int_{\mathbb{R}} W^\epsilon(x, \xi, t) \left(\int_{\mathbb{R}} e^{-i(k-\xi)y} \left(V(x + \frac{\epsilon}{2}y) - V(x - \frac{\epsilon}{2}y) \right) dy \right) d\xi . \end{aligned}$$

Now we define $Z^\epsilon(x, k)$ by

$$(3.2.4) \quad Z^\epsilon(x, k) = \frac{1}{i\epsilon} \frac{1}{2\pi} \int_{\mathbb{R}} e^{-iky} \left(V(x + \frac{\epsilon}{2}y) - V(x - \frac{\epsilon}{2}y) \right) dy ,$$

and we rewrite I as the convolution

$$I = Z^\epsilon(x, k) *_k W^\epsilon(x, k, t) .$$

Therefore, equation (3.2.3) takes the form of the integrodifferential equation

$$(3.2.5) \quad \partial_t W^\epsilon(x, k, t) + k \partial_x W^\epsilon(x, k, t) - Z^\epsilon(x, k) *_k W^\epsilon(x, k, t) = 0$$

which is known as the Wigner equation.

The Wigner equation (3.2.5) can be written in an alternative form revealing the underlying competition between the hyperbolic and dispersive character in this equation, depending on the value of the frequency ϵ . Expanding in Taylor series the potential V we observe that for small ϵ and fixed x, y we have

$$\frac{1}{\epsilon} \left(V(x + \frac{\epsilon}{2}y) - V(x - \frac{\epsilon}{2}y) \right) = yV'(x) + O(\epsilon) .$$

Then, we write $Z^\epsilon(x, k)$ in the form

$$Z^\epsilon(x, k) = -\frac{i}{2\pi} \int_{\mathbb{R}} e^{-iky} \left[\frac{V(x + \frac{\epsilon}{2}y) - V(x - \frac{\epsilon}{2}y)}{\epsilon} + yV'(x) - yV'(x) \right] dy ,$$

that is

$$(3.2.6a) \quad Z^\epsilon(x, k) = J(x, k) + \mathcal{Q}^\epsilon(x, k) ,$$

where

$$(3.2.6b) \quad J(x, k) := \left(-\frac{i}{2\pi} \int_{\mathbb{R}} e^{-iky} y dy \right) V'(x) = \partial_k \left(\frac{1}{2\pi} \int_{\mathbb{R}} e^{-iky} dy \right) V'(x) = \delta'(k) V'(x) ,$$

and

$$(3.2.6c) \quad \mathcal{Q}^\epsilon(x, k) := -\frac{i}{2\pi} \int_{\mathbb{R}} e^{-iky} \left[\frac{V(x + \frac{\epsilon}{2}y) - V(x - \frac{\epsilon}{2}y)}{\epsilon} - yV'(x) \right] dy .$$

Thus, using the formula

$$\delta'(k) *_k W^\epsilon(x, k, t) = \partial_k W^\epsilon(x, k, t) ,$$

the Wigner equation is written in the form

$$(3.2.7) \quad \partial_t W^\epsilon(x, k, t) + k \partial_x W^\epsilon(x, k, t) - V'(x) \partial_k W^\epsilon(x, k, t) = \mathcal{Q}^\epsilon(x, k) *_k W^\epsilon(x, k, t) .$$

We observe that the differential operator in left hand side of (3.2.7) is independent of the small parameter ϵ , while the convolution kernel \mathcal{Q}^ϵ in the right hand side is of order $O(\epsilon^2)$ for fixed x, k . Therefore, the formal limit of the Wigner equation as $\epsilon \rightarrow 0$ is the equation

$$(3.2.8) \quad \partial_t W(x, k, t) + k \partial_x W(x, k, t) - V'(x) \partial_k W(x, k, t) = 0 .$$

This equation is the standard Liouville equation of classical mechanics in phase space, and it is called the limit Wigner equation.

The initial data for the Wigner equation is the Wigner transform

$$(3.2.9) \quad W^\epsilon(x, k, 0) = W_0^\epsilon(x, k) = W^\epsilon[\psi_0^\epsilon](x, k) ,$$

of the initial data $\psi_0^\epsilon(x) = \psi^\epsilon(x, t = 0)$. On the other hand, the initial data for the limit Wigner equation are found by taking the limit of $W^\epsilon(x, k, 0)$ as $\epsilon \rightarrow 0$, and they have the form (cf. Section 3.1)

$$(3.2.10) \quad W_0(x, k) = |A_0(x)|^2 \delta(k - S_0'(x)) .$$

The solution of (3.2.8) is given by

$$(3.2.11) \quad W(x, k, t) = |A(x, t)|^2 \delta(k - S'(x, t))$$

with $S(x, t)$, $A(x, t)$ solutions of the eikonal and transport equations, respectively,

$$(3.2.12a) \quad S_t(x, t) + \frac{1}{2}|S_x(x, t)|^2 + V(x) = 0 , \quad S(x, t = 0) = S_0(x) ,$$

and

$$(3.2.12b) \quad (|A(x, t)|^2)_t + (|A(x, t)|S_x(x, t))_x = 0 , \quad |A(x, t = 0)|^2 = |A_0(x)|^2 ,$$

In fact, differentiating (3.2.11), and using the formula

$$f(k)\delta'(k - k_0) = -f'(k_0)\delta(k - k_0) + f(k_0)\delta'(k - k_0) ,$$

we have

$$\begin{aligned} \partial_t W(x, k, t) &= \partial_t(|A(x, t)|^2)\delta(k - \partial_x S(x, t)) - |A(x, t)|^2 \partial_x \partial_t S(x, t) \delta'(k - \partial_x S(x, t)) , \\ \partial_x W(x, k, t) &= \partial_x(|A(x, t)|^2)\delta(k - \partial_x S(x, t)) - \partial_x^2 S(x, t) |A(x, t)|^2 \delta'(k - \partial_x S(x, t)) , \\ \partial_k W(x, k, t) &= |A(x, t)|^2 \delta'(k - \partial_x S(x, t)) . \end{aligned}$$

Then,

$$\begin{aligned} k \partial_x W(x, k, t) &= k \partial_x(|A(x, t)|^2)\delta(k - \partial_x S(x, t)) - k \partial_x^2 S(x, t) |A(x, t)|^2 \delta'(k - \partial_x S(x, t)) = \\ &= \partial_x S(x, t) \partial_x(|A(x, t)|^2)\delta(k - \partial_x S(x, t)) + \partial_x^2 S(x, t) |A(x, t)|^2 \delta(k - \partial_x S(x, t)) \\ &\quad - \partial_x^2 S(x, t) \partial_x S(x, t) \delta'(k - \partial_x S(x, t)) , \end{aligned}$$

and therefore using (3.2.12a) and (3.2.12b) we have

$$\begin{aligned} \partial_t W(x, k, t) + k \partial_x W(x, k, t) - V'(x) \partial_k W(x, k, t) &= \\ &= \left(\partial_t(|A(x, t)|^2) + \partial_x S(x, t) \partial_x(|A(x, t)|^2) + \partial_x^2 S(x, t) |A(x, t)|^2 \right) \delta(k - \partial_x S(x, t)) - \\ &\quad - |A(x, t)|^2 \left(\partial_x \partial_t S(x, t) + \partial_x^2 S(x, t) \partial_x S(x, t) + V'(x) \right) \delta'(k - \partial_x S(x, t)) \\ &= \left(\partial_t(|A(x, t)|^2) + \partial_x(|A(x, t)|^2 \partial_x S(x, t)) \right) \delta(k - \partial_x S(x, t)) - \\ &\quad - |A(x, t)|^2 \left(\partial_x (\partial_t S(x, t) + \frac{1}{2} |\partial_x S(x, t)|^2 + V(x)) \right) \delta'(k - \partial_x S(x, t)) = 0 . \end{aligned}$$

It must be emphasized that for potentials of the form $V(x) = ax^2 + bx + c$, a, b, c constants, it easily follows that $\mathcal{Q}^\epsilon \equiv 0$, and therefore the Wigner equation coincides with the limit Wigner equation. These potentials are usually referred as non-essential (or non-diffractive) potentials, since the corresponding bicharacteristics are linear. In this case, only the hyperbolic character of the Wigner equation is present, and no dispersion is coming into play.

The usual mathematical analysis of the Wigner equation (3.2.5) relies on semigroup theory in Hilbert spaces, especially in L^2 , which is the natural framework of semiclassical mechanics [M]. But this context cannot be used in the numerical analysis of the particle method, which needs L^p or $W^{m,p}$ estimates, and therefore the order of convergence is related to the regularity of the potential V [AN].

4. THE PARTICLE METHOD.

4.1. The particle method for the transport equation. (Raviart [RAV])

A well-known method for solving initial value problems for transport equations of the form

$$(4.1.1) \quad \begin{cases} \frac{\partial u}{\partial t} + \sum_{i=1}^n \frac{\partial}{\partial x_i} (A_i u) + A_0 u = f, & x \in \mathbb{R}^n, t > 0 \\ u(\mathbf{x}, 0) = u_0(\mathbf{x}), \end{cases}$$

is the method of characteristics. Here $u = u(\mathbf{x}, t)$, $A_i = A_i(\mathbf{x}, t)$, $f = f(\mathbf{x}, t)$.

The characteristic curves associated with the first order differential operator $\frac{\partial}{\partial t} + \sum_{i=1}^n A_i \frac{\partial}{\partial x_i}$ are given as the solutions of the following differential system

$$(4.1.2) \quad \begin{cases} \frac{d\mathbf{X}}{dt} = a(\mathbf{X}, t), & \mathbf{X} = (X_1, \dots, X_n), \\ \mathbf{X}(s) = \mathbf{x}, & a = (a_1, \dots, a_n). \end{cases}$$

If the coefficients a_i , $0 \leq i \leq n$ and the data u_0 , f are sufficiently smooth, the problem (4.1.1) has a unique classical solution, given by

$$(4.1.3) \quad u(\mathbf{x}, t) = u_0(\mathbf{X}(0; \mathbf{x}, t)) J(0; \mathbf{x}, t) \exp\left(-\int_0^t A_0(\mathbf{X}(s; \mathbf{x}, t), s) ds\right) + \int_0^t f(\mathbf{X}(s; \mathbf{x}, t), s) J(s; \mathbf{x}, t) \exp\left(-\int_s^t A_0(\mathbf{X}(\sigma; \mathbf{x}, t) d\sigma\right) ds,$$

where $J(t; \mathbf{x}, s) = \det\left(\frac{\partial X_i}{\partial x_j}(t; \mathbf{x}, s)\right)$ is the Jacobian determinant of the transformation

$$\Phi_s^t(\mathbf{x}) = \mathbf{X}(t; \mathbf{x}, s), \quad \text{for all } s, t \in [0, T].$$

Under weaker regularity assumptions, the solution (4.1.3) can be considered as a weak solution of problem (4.1.1).

In order to construct a particle method for approximating the solution of the problem (4.1.1), it is enough to consider measure solutions (or even distributional solutions), which are defined as follows.

Definition 4.1.1 A measure $u \in \mathcal{M}(\mathbb{R}^n \times [0, T])$ is called a measure solution of (4.1.1) if

$$\begin{aligned} \langle u, L^* \phi \rangle &= \langle f, \phi \rangle + \langle u_0, \phi(\cdot, 0) \rangle, \quad \forall \phi \in C_0^1(\mathbb{R}^n \times [0, T]) \\ \text{for } u_0 &\in \mathcal{M}(\mathbb{R}^n), \quad f \in \mathcal{M}(\mathbb{R}^n \times [0, T]), \end{aligned}$$

where L^* is the formal adjoint of the linear differential operator

$$Lv = \frac{\partial v}{\partial t} + \sum_{i=1}^n \frac{\partial}{\partial x_i} (A_i v) + A_0 v.$$

The first step of a particle method for approximating weak solutions of the problem (4.1.1) is to approximate the initial condition u_0 by a linear combination of Dirac measures,

$$(4.1.4) \quad u_h^0 = \sum_{j \in J} \alpha_j \delta(\mathbf{x} - \mathbf{x}_j),$$

for some set $(\mathbf{x}_j, \alpha_j)_{j \in J}$ of points $\mathbf{x}_j \in \mathbb{R}^n$ and weights $\alpha_j \in \mathbb{R}$.

Consequently, the problem we have to solve (we consider the case of $f = 0$ for simplicity), is the following

$$(4.1.5) \quad \begin{cases} \frac{\partial u_h}{\partial t} + \sum_{i=1}^n \frac{\partial}{\partial x_i} (A_i u_h) + A_0 u_h = 0, & x \in \mathbb{R}^n, t > 0 \\ u_h(\cdot, 0) = u_h^0. \end{cases}$$

Let u_h be a measure solution of the problem (4.1.5), given by

$$(4.1.6) \quad u_h = \sum_{j \in J} \alpha_j(t) \delta(\mathbf{x} - \mathbf{X}_j(t)),$$

where $\mathbf{X}_j(t)$ and $\alpha_j(t)$ are solutions of the differential systems ($j \in J$)

$$(4.1.7) \quad \begin{cases} \frac{d}{dt} \mathbf{X}_j(t) = a(\mathbf{X}_j(t), t) \\ \mathbf{X}_j(0) = \mathbf{x}_j, \end{cases}$$

and

$$(4.1.8) \quad \begin{cases} \frac{d}{dt} \alpha_j(t) + A_0(\mathbf{X}_j(t), t) \alpha_j(t) = 0 \\ \alpha_j(0) = \alpha_j^0, \end{cases}$$

respectively. Hence for all $t \in [0, T]$, $u(\cdot, t)$ is a sum of Dirac masses whose trajectories in the (\mathbf{x}, t) space coincide with the characteristic curves passing through the points $(\mathbf{x}_j, 0)$. Such a measure solution u_h is called a particle solution of (4.1.1).

The problem that comes up first, is how to choose u_h^0 that approximates u_0 . The simplest procedure for this is the following. We cover \mathbb{R}^n with a uniform mesh of meshsize h , for some small $h > 0$. For all $j = (j_1, \dots, j_n) \in \mathbb{Z}^n$, let B_j be the cell

$$B_j = \left\{ \mathbf{x} \in \mathbb{R}^n; (j_i - \frac{1}{2})h \leq x_i \leq (j_i + \frac{1}{2})h, \quad 1 \leq i \leq n \right\}$$

where $\mathbf{x}_j = (j_i h)_{1 \leq i \leq n}$ is the center of B_j . Then, we set $u_h^0 = \sum_{j \in \mathbb{Z}^n} \alpha_j \delta(\mathbf{x} - \mathbf{x}_j)$ where α_j is an approximation of $\int_{B_j} u_0 dx$, or equivalently $\alpha_j = h^n u_0(\mathbf{x}_j)$.

In order to compute a numerical approximation of $u(\mathbf{x}, t)$ at a point (\mathbf{x}, t) , it is more useful to associate with the measure $u_h(\cdot, t)$ a continuous function $u_h^\eta(\cdot, t)$, which will approximate the function $u(\cdot, t)$ for all $t \in [0, T]$. For this we define

$$(4.1.9) \quad u_h^\eta(\mathbf{x}, t) = \sum_{j \in \mathbb{Z}^n} \alpha_j(t) \zeta_\eta(\mathbf{x} - \mathbf{X}_j(t)),$$

where $\zeta_\eta(\mathbf{x}) = \frac{1}{\eta^n} \zeta\left(\frac{\mathbf{x}}{\eta}\right)$, and $\zeta \in C^0(\mathbb{R}^n) \cap L^1(\mathbb{R}^n)$ is a "cut-off" function such that

$$\int_{\mathbb{R}^n} \zeta(\mathbf{x}) d\mathbf{x} = 1.$$

The convergence of the above described procedure for small η is asserted by the following theorem.

Theorem 4.1.1

Assume that

i) there exists an integer $k \geq 1$ such that

$$\begin{aligned} 1) & \int_{\mathbb{R}^n} \zeta(\mathbf{x}) d\mathbf{x} = 1 \\ 2) & \int_{\mathbb{R}^n} \mathbf{x}^\alpha \zeta(\mathbf{x}) d\mathbf{x} = 0, \quad \forall \alpha \in \mathbb{N}^n \text{ with } 1 \leq |\alpha| \leq k-1 \\ 3) & \int_{\mathbb{R}^n} |\mathbf{x}|^k |\zeta(\mathbf{x})| d\mathbf{x} < +\infty \end{aligned}$$

ii) $\zeta \in W^{m,\infty}(\mathbb{R}^n) \cap W^{m,1}(\mathbb{R}^n)$ for some integer $m > n$

iii) For the coefficients $a_i \in C^0(\mathbb{R}^n \times [0, T])$, $0 \leq i \leq n$, $a_1, \dots, a_n, a_0 + \text{div} a \in L^\infty(0, T; W^{l,\infty}(\mathbb{R}^n))$, $l = \max(k, m)$. Then, if $u_0 \in W^{l,p}(\mathbb{R}^n)$, there exists a constant $C = C(T) > 0$, such that for all $t \in [0, T]$

$$\|u(\cdot, t) - u_h^\eta(\cdot, t)\|_{L^p(\mathbb{R}^n)} \leq C \left\{ \eta^k \|u_0\|_{k,p,\mathbb{R}^n} + \left(\frac{h}{\eta}\right)^m \|u_0\|_{m,p,\mathbb{R}^n} \right\} . \blacksquare$$

If we replace the assumption (ii) by the assumption

iv) ζ has compact support and $\zeta \in W^{m,\infty}(\mathbb{R}^n)$ for some integer $m \geq 1$,

then, we have the following convergence theorem

Theorem 4.1.2

Under the assumptions (i),(iii),(iv), if $u_0 \in W^{l,p}(\mathbb{R}^n)$, there exists a constant $C = C(T) > 0$, such that

$$\|u(\cdot, t) - u_h^\eta(\cdot, t)\|_{L^p(\mathbb{R}^n)} \leq C \left\{ \eta^k \|u_0\|_{k,p,\mathbb{R}^n} + \left(1 + \frac{h}{\eta}\right)^{\frac{n}{q}} \left(\frac{h}{\eta}\right)^m \|u_0\|_{m,p,\mathbb{R}^n} \right\}, \quad \frac{1}{p} + \frac{1}{q} = 1 . \blacksquare$$

The last theorem does not hold if ζ belongs only to $L^\infty(\mathbb{R}^n)$. But it can be slightly improved for $m = 0, 1$, when ζ has compact support, it is piecewise smooth and it belongs to $W^{m,\infty}(\mathbb{R}^n)$. In this case, we have the following estimate

$$\|u(\cdot, t) - u_h^\eta(\cdot, t)\|_{L^\infty(\mathbb{R}^n)} \leq C \left\{ \eta^k \|u_0\|_{k,\infty,\mathbb{R}^n} + \left(1 + \frac{\eta}{h}\right)^{n-1} \left(\frac{h}{\eta}\right)^{m+1} \|u_0\|_{m+1,\infty,\mathbb{R}^n} \right\} .$$

From the above theorems it follows that $\frac{h}{\eta}$ must go to zero, as the parameters h and η go also to zero, for the particle approximation to converge. Numerical computations with the particle method for the transport equation and for a symmetric hyperbolic system have been performed by MasGallic et.al. [MG],[MR],[MP].

4.2 The particle method for the Wigner equation.

In this section, we apply the particle method for solving the Wigner equation (see Section 3.2). Following the description of the previous section, we introduce the approximation

$$(4.2.1) \quad W^\epsilon(x, k, t) = \sum_{j=1}^N a_j(t) \delta(x - x_j(t)) \delta(k - k_j(t)) \quad , \quad (x, k) \in [-a, a]x[-b, b] \quad ,$$

where $(x_j(t), k_j(t))$ is the position and the speed of j -particle at time t , and $a_j(t)$ is the weight of the j -particle, into the Wigner equation

$$(4.2.2) \quad \begin{aligned} \partial_t W^\epsilon(x, k, t) + k \partial_x W^\epsilon(x, k, t) - V'(x) \partial_k W^\epsilon(x, k, t) &= Q^\epsilon(x, k) * W^\epsilon(x, k, t) \quad , \\ W^\epsilon(x, k, 0) &= W_0^\epsilon(x, k) \quad . \end{aligned}$$

Recall that

$$(4.2.3) \quad Q^\epsilon(x, k) = \frac{-i}{2\pi} \int_{\mathbb{R}} e^{-iky} \left[\frac{V(x + y\epsilon/2) - V(x - y\epsilon/2)}{\epsilon} - yV'(x) \right] dy \quad .$$

Differentiating the particle solution (4.2.1), we have

$$\begin{aligned} \partial_t W^\epsilon(x, k, t) &= \sum_{j=1}^N \left[\dot{a}_j(t) \delta(x - x_j(t)) \delta(k - k_j(t)) \right. \\ &\quad \left. - a_j(t) \left\{ \delta'(x - x_j(t)) \dot{x}_j(t) \delta(k - k_j(t)) + \delta'(k - k_j(t)) \dot{k}_j(t) \delta(x - x_j(t)) \right\} \right] \quad , \end{aligned}$$

$$\partial_x W^\epsilon(x, k, t) = \sum_{j=1}^N a_j(t) \delta'(x - x_j(t)) \delta(k - k_j(t)) \quad ,$$

and

$$\partial_k W^\epsilon(x, k, t) = \sum_{j=1}^N a_j(t) \delta'(k - k_j(t)) \delta(x - x_j(t)) \quad .$$

Using the Hamiltonian system

$$\dot{x}_j(t) = k_j(t) \quad , \quad \dot{k}_j(t) = -V'(x_j(t))$$

the left hand side of (4.2.2) is written in the form

$$(4.2.4) \quad \partial_t W^\epsilon(x, k, t) + k \partial_x W^\epsilon(x, k, t) - V'(x) \partial_k W^\epsilon(x, k, t) = \sum_{j=1}^N \dot{a}_j(t) \delta(x - x_j(t)) \delta(k - k_j(t)) \quad ,$$

while the right hand side of (4.2.2) is written as follows

$$(4.2.5) \quad \begin{aligned} W^\epsilon(x, k, t) * Q^\epsilon(x, k) &= \int Q^\epsilon(x, k - k') W(x, k', t) dk' \\ &= \int \int Q^\epsilon(x', k - k') \zeta^\delta(x - x') W(x', k', t) dx' dk' = \sum_{j=1}^N a_j(t) Q^\epsilon(x_j(t), k - k_j(t)) \zeta^\delta(x - x_j(t)) \quad . \end{aligned}$$

Here, $\zeta^\delta(x)$ is a real function such that $\zeta^\delta(x) \rightarrow \delta(x)$, when $\delta \rightarrow 0$.

Combining (4.2.1), (4.2.4) and (4.2.5), we have

$$\sum_{j=1}^N \dot{a}_j(t) \delta(x - x_j(t)) \delta(k - k_j(t)) = \sum_{j=1}^N a_j(t) Q^\epsilon(x_j(t), k - k_j(t)) \zeta^\delta(x - x_j(t)) .$$

Then, multiplying the last equation with the test functions $\phi_\ell(x)$, $\psi_\ell(k)$ which are localized around x_ℓ and k_ℓ , respectively, and integrating with respect to x and k , we obtain

$$\sum_{j=1}^N \dot{a}_j(t) \phi_\ell(x_j(t)) \psi_\ell(k_j(t)) = \sum_{j=1}^N a_j(t) \left[\int Q^\epsilon(x_j(t), k - k_j(t)) \psi_\ell(k) dk \right] \left[\int \zeta^\delta(x - x_j(t)) \phi_\ell(x) dx \right] ,$$

which implies

$$\dot{a}_\ell(t) = \sum_{j=1}^N a_j(t) Q^\epsilon(x_j, k_\ell - k_j) \zeta^\delta(x_\ell - x_j) I_{\phi_\ell} I_{\psi_\ell} , \ell = 1 \dots N .$$

where I_ϕ denotes the length of the support of the function ϕ .

Finally, in order to determine the initial values for the position $x_j(0)$ the speed $k_j(0)$ and the weight of each particle $a_j(0)$, we use the particle representation (4.2.1) for W_0^ϵ ,

$$(4.2.8) \quad W_0^\epsilon(x, k) = \sum_j a_j(0) \delta(x - x_j(0)) \delta(k - k_j(0)) .$$

Multiplying both members of the last equation by the test functions $\phi(x)$, $\psi(k)$, and integrating with respect to x and k , we obtain

$$(4.2.9) \quad \int \int W_0^\epsilon(x, k) \phi(x) \psi(k) dx dk \approx \sum_{j=1}^N a_j(0) \phi(x_j(0)) \psi(k_j(0)) ,$$

N being the total number of particles. We approximate the above integral with a numerical integration rule, with L knots x_l , $l = 1 \dots L$ in the x -direction, and M knots k_m , $m = 1 \dots M$ in the k -direction, we have

$$(4.2.10) \quad \int \int W_0^\epsilon(x, k) \phi(x) \psi(k) dx dk \sim \sum_{\ell=1}^L \sum_{m=1}^M (\Delta x \Delta k) \beta_{\ell m} W_0^\epsilon(x_\ell, k_m) \phi(x_\ell) \psi(k_m) .$$

Comparing the approximations (4.2.9) and (4.2.10), we obtain

$$N = LM$$

$$a_j(0) = a_j^0 = (\Delta x \Delta k) \beta_{\ell m} W_0^\epsilon(x_\ell, k_m)$$

$$x_j(0) = x_j^0 = x_\ell$$

$$k_j(0) = k_j^0 = k_m$$

with $j=(m-1)L+\ell$.

Therefore, in order to construct the particle solution we must first solve the system

$$(4.2.6) \quad \begin{aligned} \dot{x}_j(t) &= k_j(t) , & x_j(0) &= x_j^0 \\ \dot{k}_j(t) &= -V'(x_j(t)) , & k_j(0) &= k_j^0 , \end{aligned}$$

and

$$(4.2.7) \quad \dot{a}_j(t) = \sum_{n=1}^N a_n(t) Q^\epsilon(k_j - k_n) \zeta^\delta(x_j - x_n) I_{\phi_j} I_{\psi_j} , \quad a_j(0) = a_j^0 .$$

Here with (x_ℓ, k_m) again we denote the knots of the integration rule with weight $\beta_{\ell m}$ while h_1 and h_2 is the discretization lengths in x and k .

In the special case of the quadratic potential $V(x) = ax^2 + bx + c$, it follows that $\dot{a}(t) = 0$, that is $a_j(t) = a_j(0)$.

Note finally that for the approximation of the Dirac mass we use the approximation sequence $\zeta^\delta(x) = \frac{1}{\delta} \zeta(\frac{x}{\delta})$ with $\zeta \in C_0^\infty$ such that $\int_{\mathbb{R}} \zeta(x) dx = 1$. In the numerical examples we will present below, we use the following cut-off functions

$$\begin{aligned} a) \quad \zeta_1(x) &= \begin{cases} \frac{1}{2}, & x \in [-1, 1] \\ 0, & \textit{otherwise} \end{cases} \\ b) \quad \zeta_2(x) &= \begin{cases} 1 - |x|, & x \in [-1, 1] \\ 0, & \textit{otherwise} \end{cases} \\ c) \quad \zeta_3(x) &= \frac{3 - 2x^2}{2\sqrt{4\pi}} \exp(-x^2) \end{aligned}$$

These functions have the following moment properties

$$\begin{aligned} \int_{\mathbb{R}} \zeta_m(x) dx &= 1 \\ \int_{\mathbb{R}} x^i \zeta_m(x) dx &= 0 , \quad m = 1, 2, 3 , \end{aligned}$$

with $i=1$ for $m = 1, 2$, and $i=2$ for $m = 3$ (cf Theorem 4.1.1).

A schematic description of the algorithm goes as follows:

- a) Place the particles according to the selected integration rule.
- b) Calculate a_j^0, x_j^0, k_j^0 , $j = 1 \dots N$
- c) Solve the system (4.2.6), (4.2.7) to find $x_j^T = x_j(T)$, $k_j^T = k_j(T)$, $a_j(T)$
- d) Calculate the sum $W^\epsilon(x, k, T) = \sum_{j=1}^N a_j(T) \zeta^\delta(x - x_j^T) \zeta^\delta(k - k_j^T)$

5 NUMERICAL EXAMPLES.

5.1 Example 1: Harmonic oscillator.

In this section we investigate the behavior of the particle method for different values of parameters like ϵ , the final time T , the number of particles N and the integration method that we use to compute the initial positions and speeds of the particles, in the case of a quadratic potential. This is a typical and interesting example, since in this case the Wigner equation coincides with the Liouville equation, and the Wigner function is computed by transporting the initial Wigner function along the bicharacteristics

5.1.1 Initial data and potential.

In our computations we use the cwith Gaussian amplitude $a_0(x) = \exp(-\frac{\lambda^2 x^2}{2})$ and quadratic phase $S_0(x) = \frac{\mu^2 x^2}{2}$ (λ, μ positive constants). Applying the Wigner transform to $\Psi_0^\epsilon(x)$ we compute the initial Wigner function

$$(5.1.2) \quad W_0^\epsilon(x, k) = \frac{1}{\sqrt{\pi}} \frac{e^{-\lambda^2 x^2}}{\lambda \epsilon} \exp\left(-\frac{(k - \mu^2 x)^2}{(\lambda \epsilon)^2}\right), \quad (x, k) \in \mathbb{R}_{xk}^2.$$

The potential has the form

$$(5.1.3) \quad V(x) = \frac{\Omega^2 x^2}{2},$$

Ω being a positive constant (the frequency of the harmonic oscillator). For this potential we can solve explicitly the corresponding Hamiltonian system to find the bicharacteristics

$$(5.1.4) \quad \begin{aligned} x(q, p, t) &= q \cos(\Omega t) + \frac{p}{\Omega} \sin(\Omega t), \\ k(q, p, t) &= -q\Omega \sin(\Omega t) + p \cos(\Omega t). \end{aligned}$$

Solving for the initial position q and momentum p , and substituting into W_0^ϵ , we obtain the Wigner function (see, e.g., Kalligiannaki [KAL])

$$(5.1.5) \quad W^\epsilon(x, k, t) = W_0^\epsilon\left(x \cos(\Omega t) - \frac{k}{\Omega} \sin(\Omega t), x\Omega \sin(\Omega t) + k \cos(\Omega t)\right).$$

5.1.2 Integration methods.

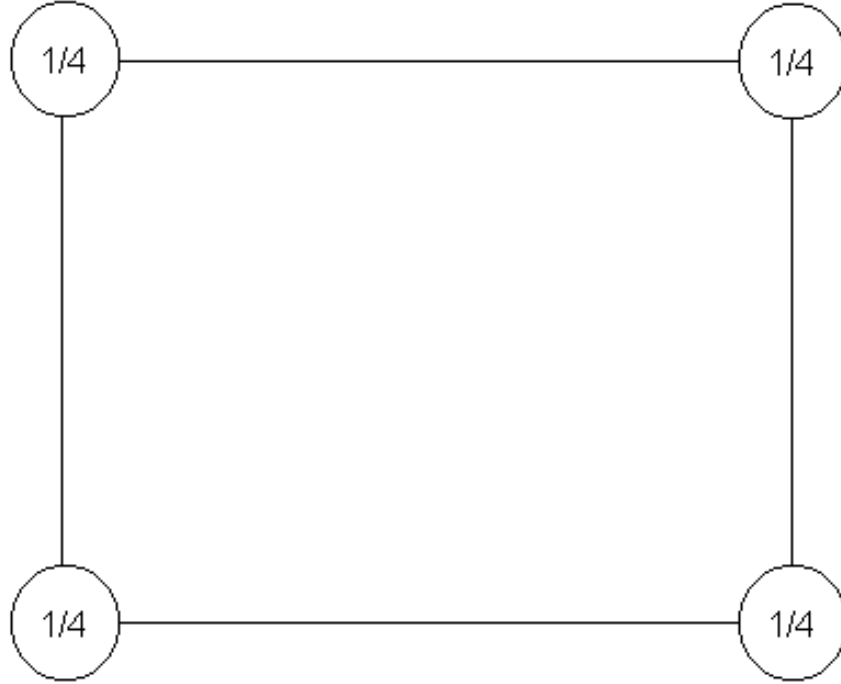
a. Trapezoid method.

The simplest method to place the particles is the trapezoid method. Dividing the original box into L smaller boxes in the direction of x and M boxes to the direction of k each with dimensions $\Delta x = \frac{2a}{L-1}$, $\Delta k = \frac{2b}{M-1}$ we obtain LM knots

$$\begin{aligned} x_\ell &= -a + (\ell - 1)\Delta x, \quad \ell = 1 \dots L, \\ k_m &= -b + (m - 1)\Delta k, \quad m = 1 \dots M. \end{aligned}$$

Each of the knots that belong to one of the smaller boxes has the same weight $1/4$ so the knots that belong to two boxes have a weight of $1/2$ and those that belong to four boxes have a weight of

$$\beta_{\ell m} = \begin{cases} 1/4, & (\ell, m) = (1, 1), (1, M), (L, 1), (L, M) \\ 1/2, & (\ell, m) = (1, 2 \dots M - 1), (L, 2 \dots M - 1), (2 \dots L - 1, 1), (2 \dots L - 1, M) \\ 1, & \text{otherwise} \end{cases}$$

FIGURE 1 *Weights for the trapezoid method*

The initial position and weight of the LM particles are given by

$$a_j^0 = (\Delta x \Delta k) \beta_{\ell m} W_0^\epsilon(x_\ell, k_m)$$

$$x_j^0 = x_\ell$$

$$k_j^0 = k_m$$

with $j=(m-1)L+\ell$. This is the method with the lowest accuracy since it can integrate exactly polynomials of first degree in respect of x and k .

b. Simpson method.

The second method we used is the Simpson method. Again we break the original box in the same way to LM smaller boxes, placing nine knots in each of the smaller boxes. Four of the knots are placed at the corners with a weight of $1/36$, four knots are placed between the corners with a

weight of $1/9$ and finally one knot is placed in the center of the box with a weight of $4/9$. The total number of knots is $\tilde{L}\tilde{M}$ with $\tilde{L} = 2L - 1$ and $\tilde{M} = 2M - 1$. The position of the knots is given by

$$x_\ell = -a + (\ell - 1)\frac{\Delta x}{2}, \ell = 1 \dots \tilde{L}$$

$$k_m = -b + (m - 1)\frac{\Delta k}{2}, m = 1 \dots \tilde{M}$$

and their weight is given by

$$\begin{aligned} \beta_{\ell m} &= 1/36 \quad \text{for } (\ell, m) = (1, 1), (1, \tilde{M}), (\tilde{L}, 1), (\tilde{L}, \tilde{M}) \\ \beta_{\ell m} &= 1/18 \quad \text{for } \ell = 3, 5, \dots, \tilde{L} - 2, \quad m = 1, m = \tilde{M} \\ \beta_{\ell m} &= 1/9 \quad \text{for } \ell = 2, 4, \dots, \tilde{L} - 1, \quad m = 1, m = \tilde{M} \\ \beta_{\ell m} &= 1/18 \quad \text{for } m = 3, 5, \dots, \tilde{M} - 2, \quad \ell = 1, \ell = \tilde{L} \\ \beta_{\ell m} &= 1/9 \quad \text{for } m = 2, 4, \dots, \tilde{M} - 1, \quad \ell = 1, \ell = \tilde{L} \\ \beta_{\ell m} &= 1/9 \quad \text{for } \ell = 3, 5, \dots, \tilde{L} - 2, \quad m = 3, 5, \dots, \tilde{M} - 2 \\ \beta_{\ell m} &= 4/9 \quad \text{for } \ell = 2, 4, \dots, \tilde{L} - 1, \quad m = 2, 4, \dots, \tilde{M} - 1 \\ \beta_{\ell m} &= 2/9 \quad \text{for } \ell = 3, 5, \dots, \tilde{L} - 2, \quad m = 2, 4, \dots, \tilde{M} - 1 \\ \beta_{\ell m} &= 2/9 \quad \text{for } \ell = 2, 4, \dots, \tilde{L} - 1, \quad m = 3, 5, \dots, \tilde{M} - 2 \end{aligned}$$

The initial position and the weight of each particle is given by

$$a_j^0 = (\Delta x \Delta k) \beta_{\ell m} W_0^\epsilon(x_\ell, k_m)$$

$$x_j^0 = x_\ell$$

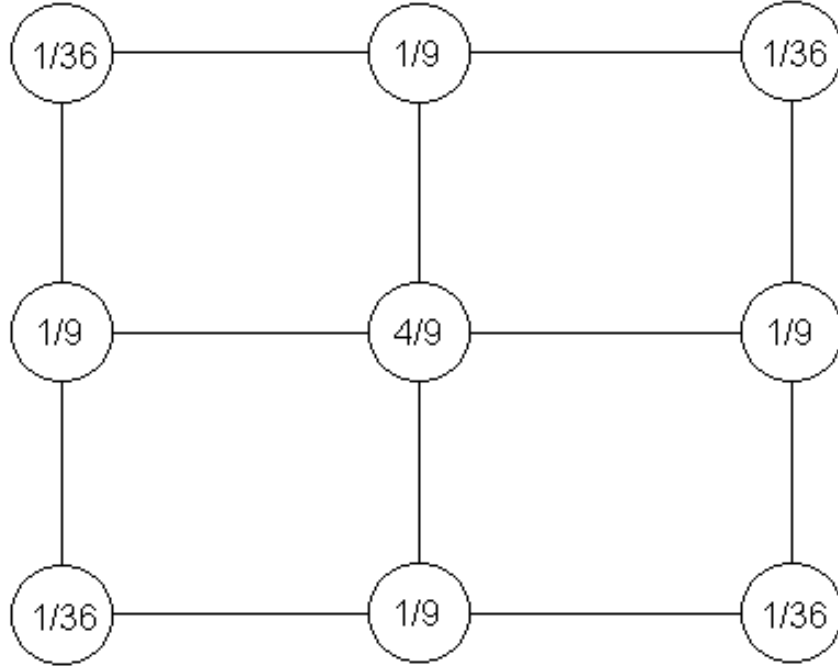
$$k_j^0 = k_m$$

with $j = (m - 1)\tilde{L} + \ell$. The Simpson method can integrate exactly polynomials of third degree in respect of x and k .

c. Gauss-Legendre method.

The third method we used is the Gauss Legendre method of third degree. Again we break the large box to L boxes in the direction of x and to M boxes in the direction of k but now we place nine knots in the interior of each of the smaller boxes for a total number of knots of $3(L-1)3(M-1) = \tilde{L}\tilde{M}$. If the (ℓ, m) box has coordinates $[x_\ell, x_{\ell+1}] \times [k_m, k_{m+1}]$ then the coordinates of the particles that are initially inside it are given by

$$\begin{aligned} x_j^0 &= \frac{x_\ell + x_{\ell+1}}{2} - \frac{\Delta x}{2} \sqrt{\frac{3}{5}}, \quad \text{for } \hat{i} = 1 \\ x_j^0 &= \frac{x_\ell + x_{\ell+1}}{2}, \quad \text{for } \hat{i} = 2 \\ x_j^0 &= \frac{x_\ell + x_{\ell+1}}{2} + \frac{\Delta x}{2} \sqrt{\frac{3}{5}}, \quad \text{for } \hat{i} = 3 \\ k_j^0 &= \frac{k_m + k_{m+1}}{2} - \frac{\Delta k}{2} \sqrt{\frac{3}{5}}, \quad \text{for } \hat{i} = 1 \\ k_j^0 &= \frac{k_m + k_{m+1}}{2}, \quad \text{for } \hat{i} = 2 \\ k_j^0 &= \frac{k_m + k_{m+1}}{2} + \frac{\Delta k}{2} \sqrt{\frac{3}{5}}, \quad \text{for } \hat{i} = 3 \end{aligned}$$

FIGURE 2. *Weights for the Simpson method*

and their weights by

$$\beta_{i,\hat{i}} = \begin{cases} 64/324, & (i, \hat{i}) = (2, 2) \\ 40/324, & (i, \hat{i}) = (1, 2), (2, 1), (2, 3), (3, 2) \\ 25/324, & (i, \hat{i}) = (1, 1), (3, 3), (1, 3), (3, 1) \end{cases}$$

$$a_j^0 = (\Delta x \Delta k) \beta_{i,\hat{i}} W_0^c(x_j^0, k_j^0)$$

with

$$j = 9(L - 1)(m - 1) + 9(\ell - 1) + 3(i - 1) + \hat{i}.$$

This method is the most accurate of those we used since it can integrate exactly polynomials of fifth degree in respect of x and k .

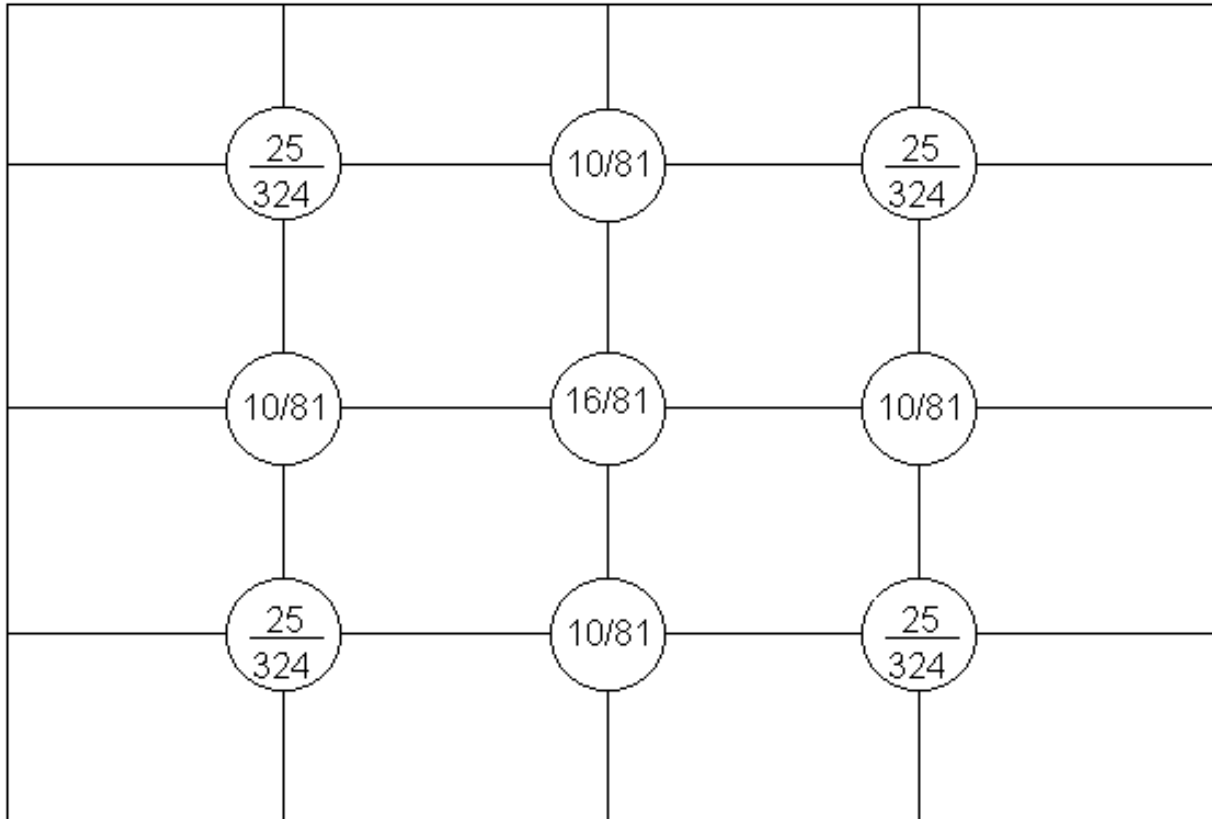


FIGURE 3 *weights for the Gauss – Legendre method*

5.1.3 Numerical results.

In this section we will compare the particle solution with the analytical solution of the Wigner equation for different values of the physical and numerical parameters. For the implementation of the method we used the following arithmetical values for our parameters $a = 3.2$, $b = 10$, $\delta = 0.2$,

$\lambda = 1.5$, $\mu = 1$, $\Omega = \pi$, and for the approximation of the Dirac mass we used the hut function.

In Figures 4-6 we show the variation of the L_2 norm of the error wrt. time for the three integration rules we used to initialize the particles. The number of particles is approximately 24300 and the value of ϵ varies from 0.25 to 1 with a step of 0.25. We observe that the error has a periodical behavior with a period of 1 which is equal to the period of the analytical solution. In Figures 7-9 we show the error for the three methods wrt. the number of particles for final time $T=2$ and for $\epsilon = 0.1, 0.25, 0.4, 1$. We observe that the error falls initially as the number of particles decreases to reach a minimum around 20.000 - 40.000 particles, depending on the integration rule, and it then slowly starts to increase as the number of particles increases. Finally, as we expect, for a fixed number of particles and a fixed final time, the error increases as $\epsilon \rightarrow 0$.

As we mentioned before the particle method requires a large number of calculations in order to calculate the solution through $W^\epsilon(x, k, T) = \sum_j^N a_j^0 \zeta^\delta(x - x_j^T) \zeta^\delta(k - k_j^T)$ when N is large. The number of calculations reduces using the fact that $\zeta^\delta(x)$ has compact support around zero, so if we want to calculate the solution at some points (x_i, k_i) instead of summing over all the particles we only sum over those particles that satisfy $|x_i - x_j| < \delta$ and $|k_i - k_j| < \delta$ where δ is length of the support of $\zeta^\delta(x)$

5.1.4 Particle in cell (PIC) methods.

An alternative strategy to reduce the huge amount of calculations that are required in the particle method is to apply the so-called the particle in cell method (P.I.C).

Regarding the computation of a_j^0 , and x_j^T, k_j^T by solving the Hamiltonian the method is exactly the same as the standard one. However instead of calculating the sum (4.2.1), we create a new grid with $\dim X$ knots in the x -direction and $\dim K$ in the k -direction on which we are going to calculate the solution, and then, the weight of each particle $a_j(t) = a_j^0$ is distributed between the four knots of the box containing the particle. More precisely, the weight is multiplied by a factor of $\frac{1}{\delta^2}$, since the representation

$$W^\epsilon(x, k, t) = \sum_j a_j(t) \zeta^\delta(x - x_j(t)) \zeta^\delta(k - k_j(t)) ,$$

implies

$$W^\epsilon(x_i(t), k_i(t), t) = \frac{1}{\delta^2} a_i(t) .$$

If we denote by $W(i, \hat{i})$ the approximation at the knot $(-a + (i - 1)\Delta x, -b + (\hat{i} - 1)\Delta k)$, $i = 0 \dots \dim X + 1$, $\hat{i} = 0 \dots \dim K + 1$, and (i, \hat{i}) the box $[-a + (i - 1)\Delta x, -a + i\Delta x] \times [-b + (\hat{i} - 1)\Delta k, -b + \hat{i}\Delta k]$, then the j particle belongs to the box with

$$i = \left\lceil \frac{x_j^0 + \acute{a}}{\Delta x} \right\rceil , \quad \hat{i} = \left\lceil \frac{k_j^0 + \acute{b}}{\Delta k} \right\rceil ,$$

with

$$\Delta x = \frac{2a}{\dim X - 1} , \quad \Delta k = \frac{2b}{\dim K + 1} .$$

for the particles with $|x_j^0| \leq \acute{a}$, $|k_j^0| \leq \acute{b}$ with $\acute{a} = a + \Delta x$, $\acute{b} = b + \Delta k$. This extension of the domain has been done in order to include a part of the weight of the particles that lie in the boundary zone outside $[-a, a] \times [-b, b]$. The contributions of the j particle in each of the corners of its box are given by the following equations

$$\begin{aligned} \frac{1}{\delta^2} a_j^0 \frac{\epsilon_3}{\Delta x \Delta k} &\Rightarrow W(i, \hat{i}) \quad , \epsilon_3 = \left[-a + i\Delta x - x_j^0 \right] \left[-b + \hat{i}\Delta k - k_j^0 \right] \\ \frac{1}{\delta^2} a_j^0 \frac{\epsilon_4}{\Delta x \Delta k} &\Rightarrow W(i + 1, \hat{i}) \quad , \epsilon_4 = \left[x_j^0 + a - (i - 1)\Delta x \right] \left[-b + \hat{i}\Delta k - k_j^0 \right] \\ \frac{1}{\delta^2} a_j^0 \frac{\epsilon_2}{\Delta x \Delta k} &\Rightarrow W(i, \hat{i} + 1) \quad , \epsilon_2 = \left[-a + i\Delta x - x_j^0 \right] \left[k_j^0 + b - (\hat{i} - 1)\Delta k \right] \\ \frac{1}{\delta^2} a_j^0 \frac{\epsilon_1}{\Delta x \Delta k} &\Rightarrow W(i + 1, \hat{i} + 1) \quad , \epsilon_1 = \left[x_j^0 + a - (i - 1)\Delta x \right] \left[k_j^0 + b - (\hat{i} - 1)\Delta k \right] \end{aligned}$$

After computing all the $W(i, \hat{i})$, we can keep the values of $i = 1 \dots \dim X$, $\hat{i} = 1 \dots \dim K$ that correspond to the original domain $[-a, a] \times [-b, b]$.

5.1.5 Numerical results for the PIC method.

In this paragraph we compare the numerical solution computed by using the PIC method with the analytical solution. For the comparison of the PIC method with the standard particle method we show the same quantities, and we use the same values for the parameters, $a = 3.2$, $b = 10$, $\lambda = 1.5$, $\mu = 1$, $\Omega = \pi$ and for $\Delta x = \Delta k = 0.2$.

In Figures 10-12 we show the error for the three PIC methods with respect to δ and $\epsilon = 1$. A simple way to determine the correct value of δ is to compare our initial data with the solution computed by the P.I.C algorithm for final $T = 0$ since changes in δ only change the scaling of the numerical solution. In both ways the minimum error is obtained for $\delta = \Delta x = \Delta k$

In Figures 13-15 we show the error for the three methods wrt. time for $\epsilon = 0.25$, $\epsilon = 0.5$, $\epsilon = 0.75$, $\epsilon = 1$. Again like the standard particle method the error shows a periodic behavior which coincides with the period of the analytical solution. Finally, in Figures 16-18 we have the error over the particle number for $\epsilon = 0.1$, 0.15 , 0.25 , 0.5 , 1 . The error again falls to reach a minimum at around 10.000 particles, and then increases slowly. Comparing the standard particle method with PIC one, for the same final time $T=2$ and $\epsilon = 0.1$, we see that the standard particle method reaches a minimum L_2 norm of error about 0.6 while the P.I.C has a minimum L_2 norm of error about 0.8 . Both methods attain their minimum error around 10.000 particles.

The P.I.C method greatly reduce the calculations needed for the simple particle method since the weight of each particle contributes only to the four points of the box that include it.

5.2 Example 2: Quartic oscillator.

In this section we apply the particle in cell method for solving the Wigner equation for the case of quartic potential $V(x) = x^4/4$. Since the analytical solution of the Wigner equation is not known in this case, we compute the amplitude $|\psi_\epsilon|$ of the solution of Schrödinger equation derived by k -integration of the Wigner function, with that derived by FEM computation.

5.2.1 The convolution term.

In the case of a quartic potential, the convolution term in the Wigner equation reduces to a third-order dispersive (with respect to k), since the kernel Q^ϵ has the form

$$Q^\epsilon(x, k) = -\epsilon^2 x \delta'''(k)/4 .$$

Therefore in the particle approximation we have the term

$$\partial_k^3 W^\epsilon(x, k, t) = \sum_{j=1}^N a_j(t) \delta'''(k - k_j(t)) \delta(x - x_j(t)) .$$

In the numerical computation, for the approximation of the third derivative of the Dirac function we differentiate the approximating sequence (cf Chertock and Levy [CHL]).

5.2.2 Numerical results for the quartic oscillator.

Recall that since for the quartic potential we do not know the analytical solution of the Wigner equation, in order to examine the accuracy of the P.I.C method we compare the numerical results for the energy density obtained by integrating with respect to k the P.I.C solution of the Wigner equation, with the density computed by a finite element method code.

As in the first example we set $\lambda = 1.5$ and $\mu = 1$. The solution was calculated on a normal grid with $\Delta x = \Delta k = 0.1$ while the scaling factor δ of the particle weight was set equal with the discretization length for the same reasons we saw in the first example. Finally for the placement of the particles we used the trapezoid method since the results we took using each method had very small differences.

In Figure 16 we show the PIC solution for $T = 1$ and $\epsilon = 1$. The computational domain is $[-4,4] \times [-4,4]$ and we use about 25.000 particles. In Figures 20-23 we compare the results of the FEM and the PIC method for time $T = 0.6$ and about 57.000 particles, and for $\epsilon = 1, 0.5, 0.25, 0.1$ respectively. In this case the computational domain is again $[-4,4] \times [-4,4]$. In these four graphs we observe that the two methods give almost the same results.

In Figures 24-29 we observe that for the same $T=0.6$ and for ϵ between 0.1 and 1 we can obtain the same accuracy using much less particles. More specifically in Figures 24-26, we see that for 3600 particles and for $\epsilon = 1, 0.25, 0.1$, respectively, the P.I.C solution shows an oscillatory behavior especially near $x = 0$. These oscillations can be removed if we increase the number of particles. For example, in Figures 27 and 28 we have the same cases as in Figures 24 and 25 for 10.000 particles, and in Figure 29 the same case as in Figure 26, but with 14.400 particles. Further increase of the number of particles, increase the accuracy and the smoothness of the solution but it also tremendously increases the computational time.

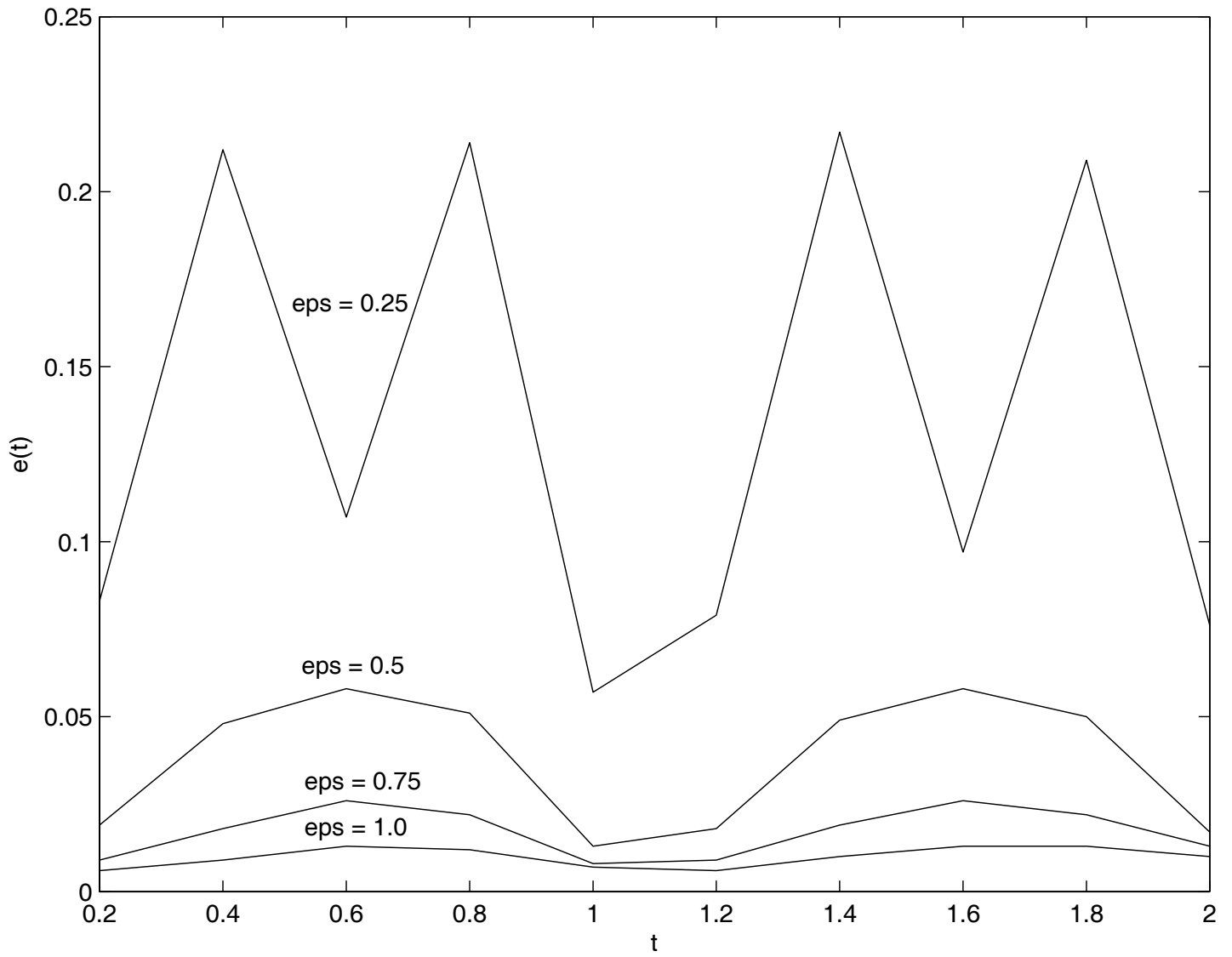
In the contrary to the case of harmonic oscillator, when we try to compute the P.I.C solution for larger times, we see that the two methods start to show up large differences, as we can see, for example, in Figures 30-32 where we compare the two methods for $T=1$ and for 57.600 particles and $\epsilon = 1, 0.25, 0.1$.

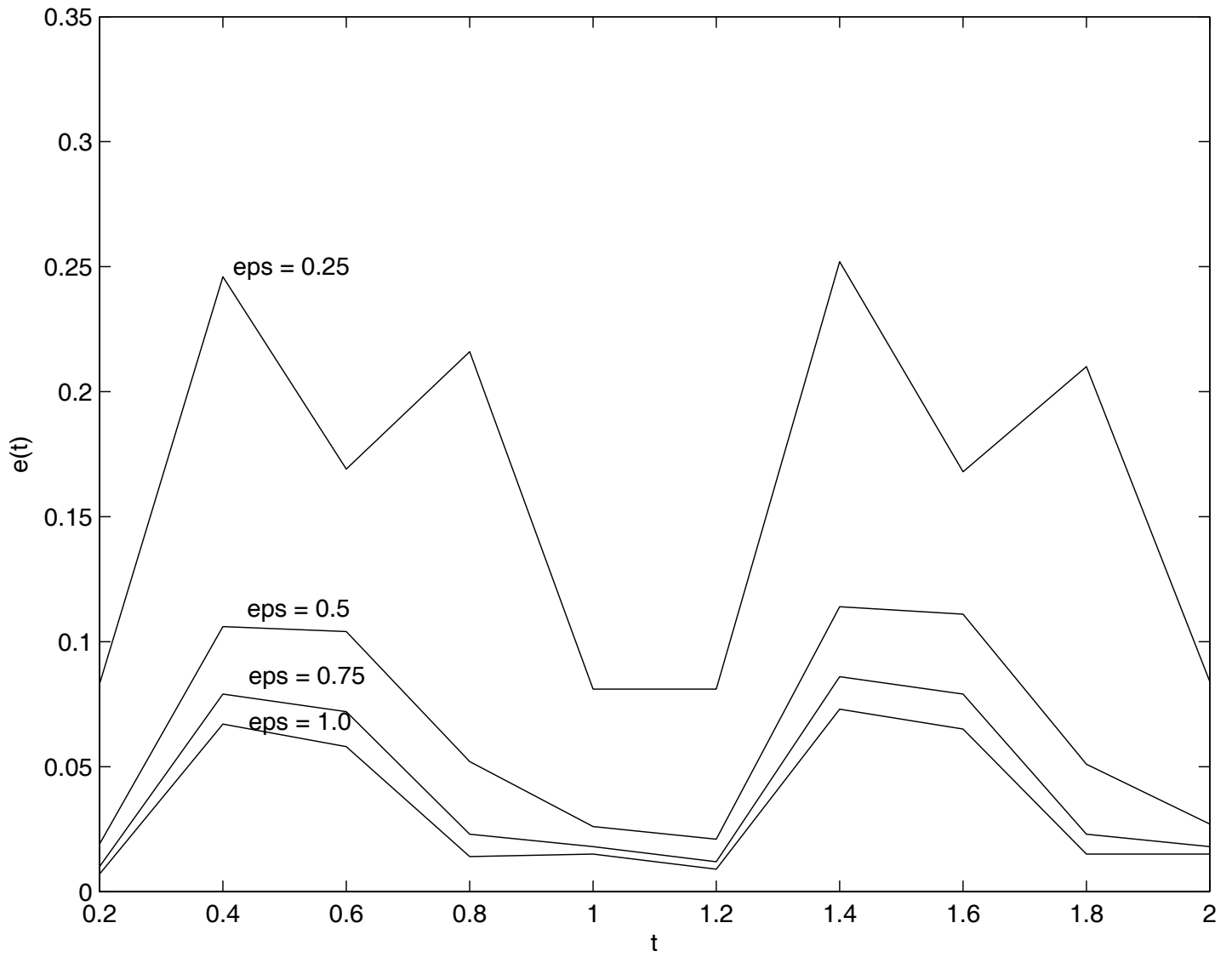
REFERENCES

- [AD] G.D. Akrivis and V.A. Dougalis, *On a class of conservative highly accurate Galerkin methods for the Schrödinger equation*, Math. Notes Num. Anal. **25(6)** (1991), 643-670.
- [AN] A. Arnold and F. Nier, *Numerical analysis of the deterministic particle method applied to the Wigner equation*, Math. Comp. **58(198)** (1992), 645-669.
- [ARN1] V.I. Arnold, *Integrals of rapidly oscillating functions and singularities of projections of Lagrangian manifolds*, Func. Anal. Appl. **6(3)** (1972), 222-224.
- [ARN2] V.I. Arnold, *Characteristic class entering in quantization conditions*, Func. Anal. Appl. **1(1)** (1967), 1-13.
- [BB] V.B. Babich and V.S. Buldyrev, *Short-Wavelength Diffraction Theory. Asymptotic Methods*, Springer-Verlag, Berlin-Heidelberg, 1991.
- [BK] V.M. Babich and N.Y. Kirpichnikova, *The Boundary-Layer Method in Diffraction Problems*, Springer-Verlag, Berlin-Heidelberg, 1979.
- [BLP] A. Bensoussan, J.-L. Lions and G. Papanicolaou, *Asymptotic Analysis for Periodic Structures*, North-Holland, Amsterdam-New York-Oxford, 1978.
- [BKP] J.D. Benamou, T. Katsaounis and B. Perthame, *High frequency Helmholtz equation, geometrical optics and particle methods*, Revist. Math Iberoam. **18(1)** (2002), 187-209.
- [CHL] A. Chertock and D. Levy, *Particle Methods for Dispersive Equations*, J. Comp. Pys **171** (2001), 708-730.
- [COL] M.D. Collins, *Nearfield asymptotic analysis for underwater acoustics*, S. Acoust.Soc. Am. **85(7)** (1989), 1107-1114.
- [CPR] F. Castella, B. Perthame and O. Runborg, *High frequency limit of the Helmholtz equation II: source on a general smooth manifold*, Comm. Partial Diff. Equ. **27(3-4)** (2002), 607-651.
- [ER] B. Engquist and O. Runborg, *Multi-phase computations in geometrical optics*, J. Comp. Appl. Math. **74** (1996), 175-192.
- [FL] S. M. Flattè, *The Schrödinger equation in classical physics*, Am. J. Phys. **54(12)** (1986), 1088-1092.
- [FM] S. Filippas and G.N. Makrakis, *Semiclassical Wigner function and Geometrical Optics*, SIAM Multi-scale Modeling and Simulation **1(4)** (2003), 674-710.
- [GM] I. Gasser and P.A. Markowich, *Quantum hydrodynamics, Wigner transform and the classical limit*, Asympt. Anal **14** (1997), 97-116.
- [GMMP] P. Gerard, P.A. Markowich, N.J. Mauser and F. Poupaud, *Homogenization limits and Wigner transforms*, Comm. Pure Appl. Math. **50** (1997), 323-380.
- [JL] Shi Jin & Xiantao Li, *Multi-phase computations of the semiclassical limit of the Schrödinger equation and related problems: Whitham vs. Wigner*, Phys. D **182(1-2)** (2003), 46-85.
- [KAL] E. Kalligiannaki, *Particle method for the Wigner equation in high-frequency paraxial propagation*, Master Thesis, Dept. Mathematics, Univ. Crete, 2002.
- [KO1] Yu. A. Kravtsov and Yu.I. Orlov, *Caustics, Catastrophes and Wave Fields*, Springer Series on Wave Phenomena, Springer-Verlag, Berlin, 1993.
- [KO2] Yu.A. Kravtsov and Yu.I. Orlov, *Geometrical Optics of Inhomogeneous Media*, Springer Series on Wave Phenomena 6, Springer-Verlag, Berlin, 1990.
- [LEE] D. Lee, *Parabolic equation development in the twentieth century*, J. Comp. Acoust. **8(4)** (2000), 527-637.
- [LP] P.L. Lions and T. Paul, *Sur les mesures de Wigner*, Rev. Math. Iberoamericana **9** (1993), 563-618.
- [M] P. Markowich, *On the equivalence of the Schrödinger and the quantum Liouville equation*, Math. Meth. Appl. Sci. **11** (1989), 459-469.
- [MA] N. Markovitz, *Quasiparticle view of wave propagation*, Proc. IEEE **68(11)** (1980), 1380-1395.
- [MG] S. Mas-Gallic, *A deterministic particle method for the linearized Boltzmann equation*, Transport theory and Statistical Physics **16(4-6)** (1987), 855-887.
- [MP] S. Mas-Gallic and F. Poupaud, *Approximation of the transport equation by a weighted particle method*, Transport theory and Statistical Physics **17(4)** (1988), 311-345.
- [MR] S. Mas-Gallic and P.A. Raviart, *A particle method for first order symmetric systems*, Numer.Math. **51** (1987), 323-352.
- [N] F. Nier, *Etude mathématique et numérique de modèles cinétiques quantiques issus de la physique des semi-conducteurs*, Ph.D. Thesis, .
- [PR] G Papanicolaou and L. Ryzhik, *Hyperbolic equations and Frequency Interactions (Eds. L. Caffarelli and E. Weinan)*, IAS/ Park City Mathematical Series, AMS, 1999.
- [RAV] P.A. Raviart, *An analysis of particle methods*, Lecture Notes in Mathematics **1127** (1983), Springer, 245-323.

- [RU] O. Runborg, *Some new results in multiphase geometrical optics* *jour Math. Model. Num. Anal.* **34(6)** (2000), 1203-1231.
- [TAP1] F. D. Tappert, *Wave Propagation and Underwater Acoustics (Eds.J.B. Keller and J.S. Papadakis)* *Lecture Notes in Physics, Vol. 70*, Springer, Berlin, 1977.
- [TAP2] F. D. Tappert, *Diffraction ray tracing of laser beams*, *J. Opt. Soc. Am.* **66(12)** (1976), 1368-1373.
- [TAT2] V.I. Tatarskii, *The Wigner representation of quantum mechanics*, *Sov. Phys. Usp.* **26(4)** (1984), 311-327.
- [TAT1] V.I. Tatarskii, *The Effects of the Turbulent Atmosphere on Wave Propagation*, Israel Program for Scientific Translation, Jerusalem, 1971.
- [WIG] E. Wigner, *On the quantum correction for thermodynamic equilibrium*, *Phys. Rev.* **40** (1932), 749-759.

**HARMONIC OSCILLATOR. STANDARD PARTICLES.
VARIATION OF THE L_2 NORM OF THE ERROR vs.
TIME (Figs. 4-6) and NUMBER OF PARTICLES (Figs. 7-9)**

FIGURE 4. *Harmonic oscillator, trapezoid integration*

FIGURE 5. *Harmonic oscillator, Simpson integration.*

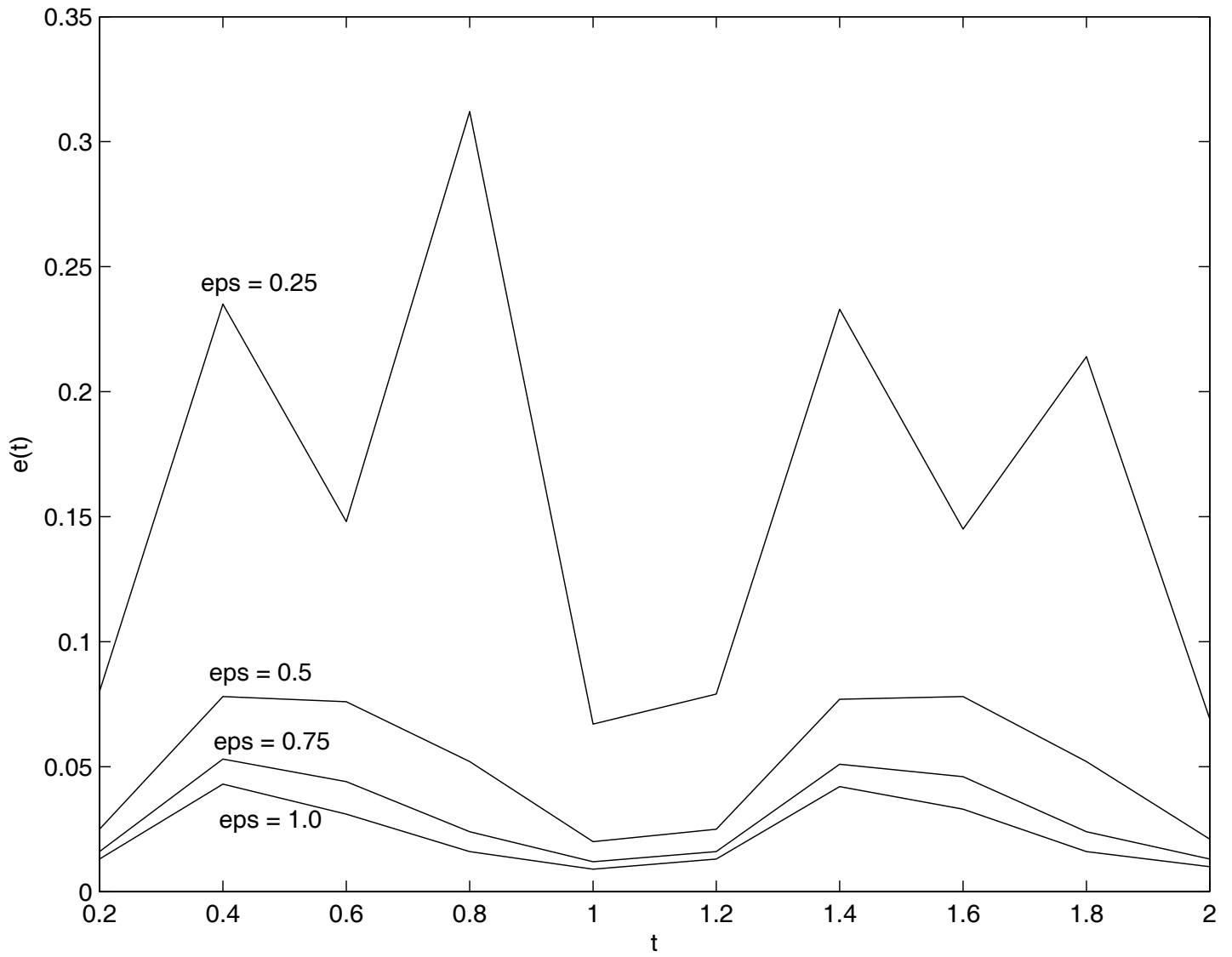


FIGURE 6. *Harmonic oscillator, Gauss – Legendre integration.*

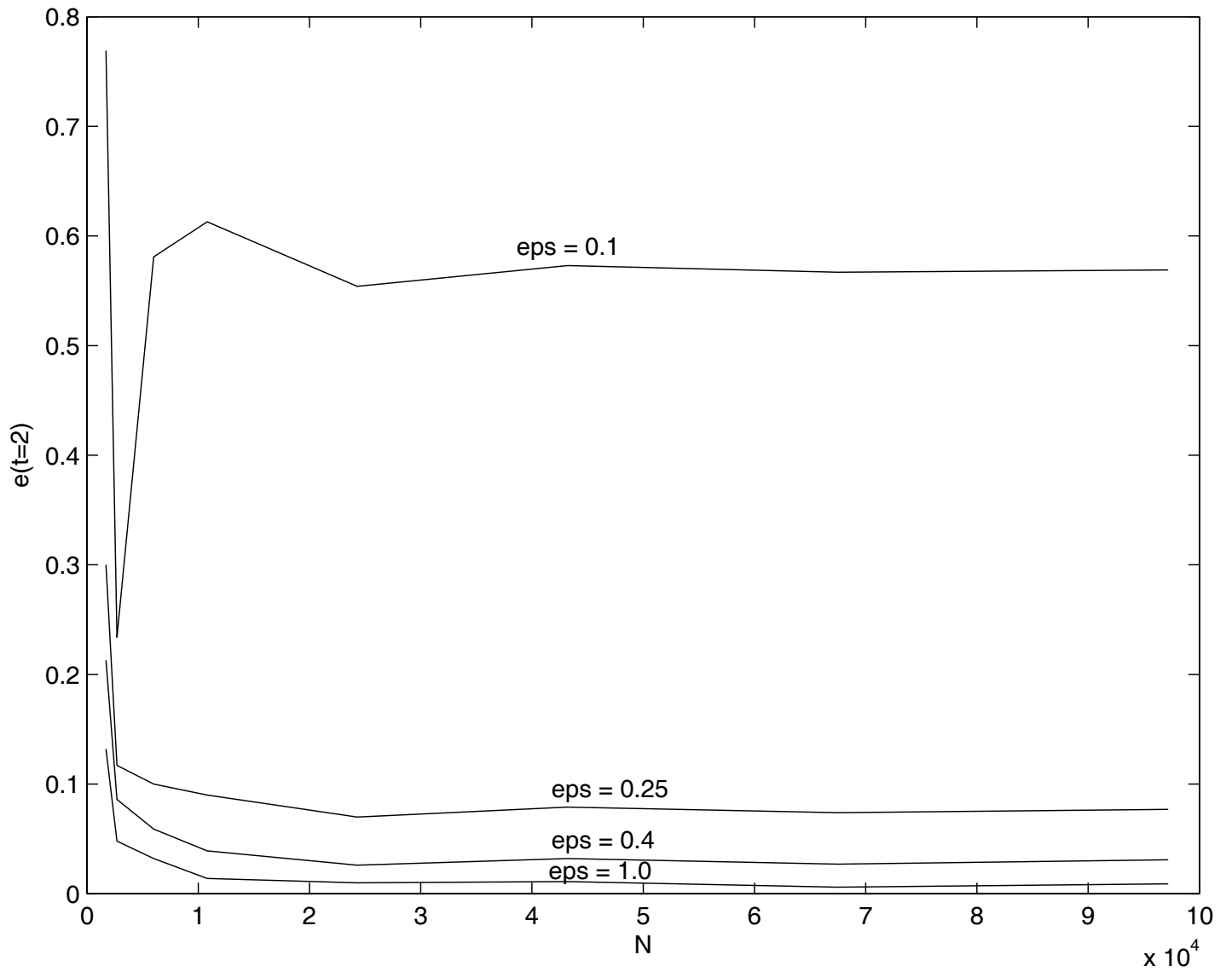
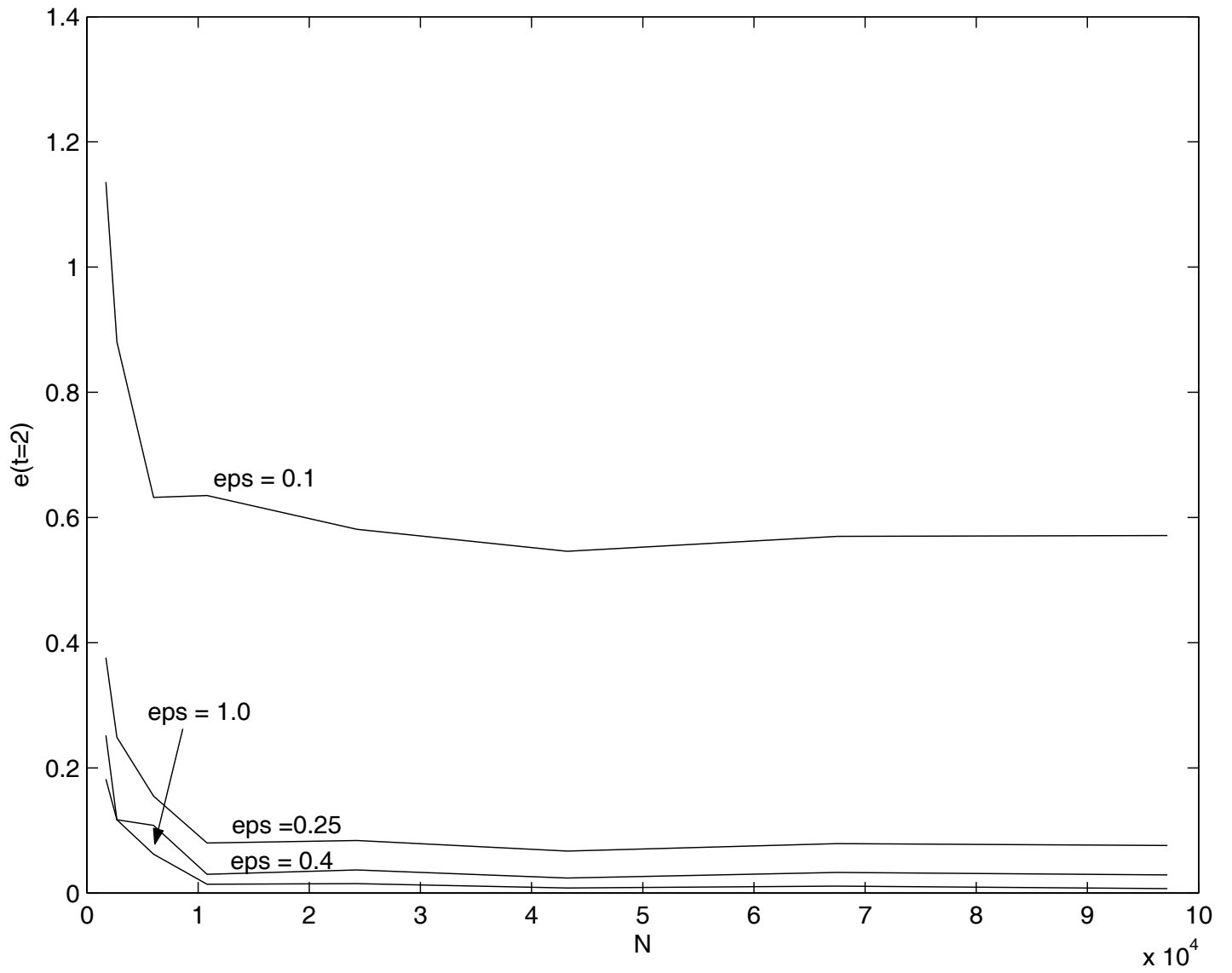
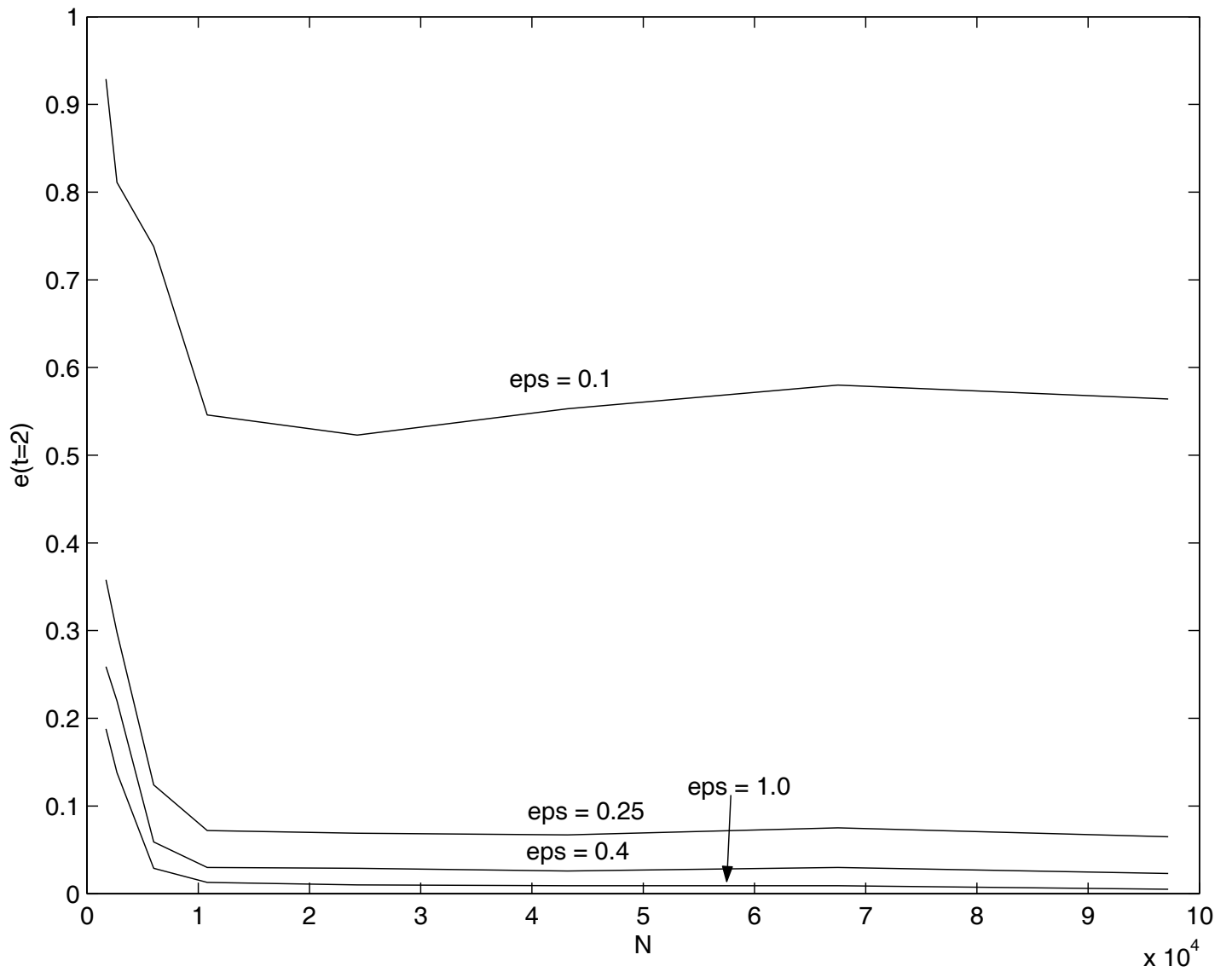


FIGURE 7. *Harmonic oscillator, trapezoid integration.*

FIGURE 8. *Harmonic oscillator, Simpson integration.*

FIGURE 9. *Harmonic oscillator, Gauss – Legendre integration.*

**HARMONIC OSCILLATOR. PARTICLE-IN-CELL.
VARIATION OF THE L_2 NORM OF THE ERROR vs.
PARAMETER δ (Figs. 10-12), TIME (Figs. 13-15) and NUMBER OF PARTICLES (Figs. 16-18).**

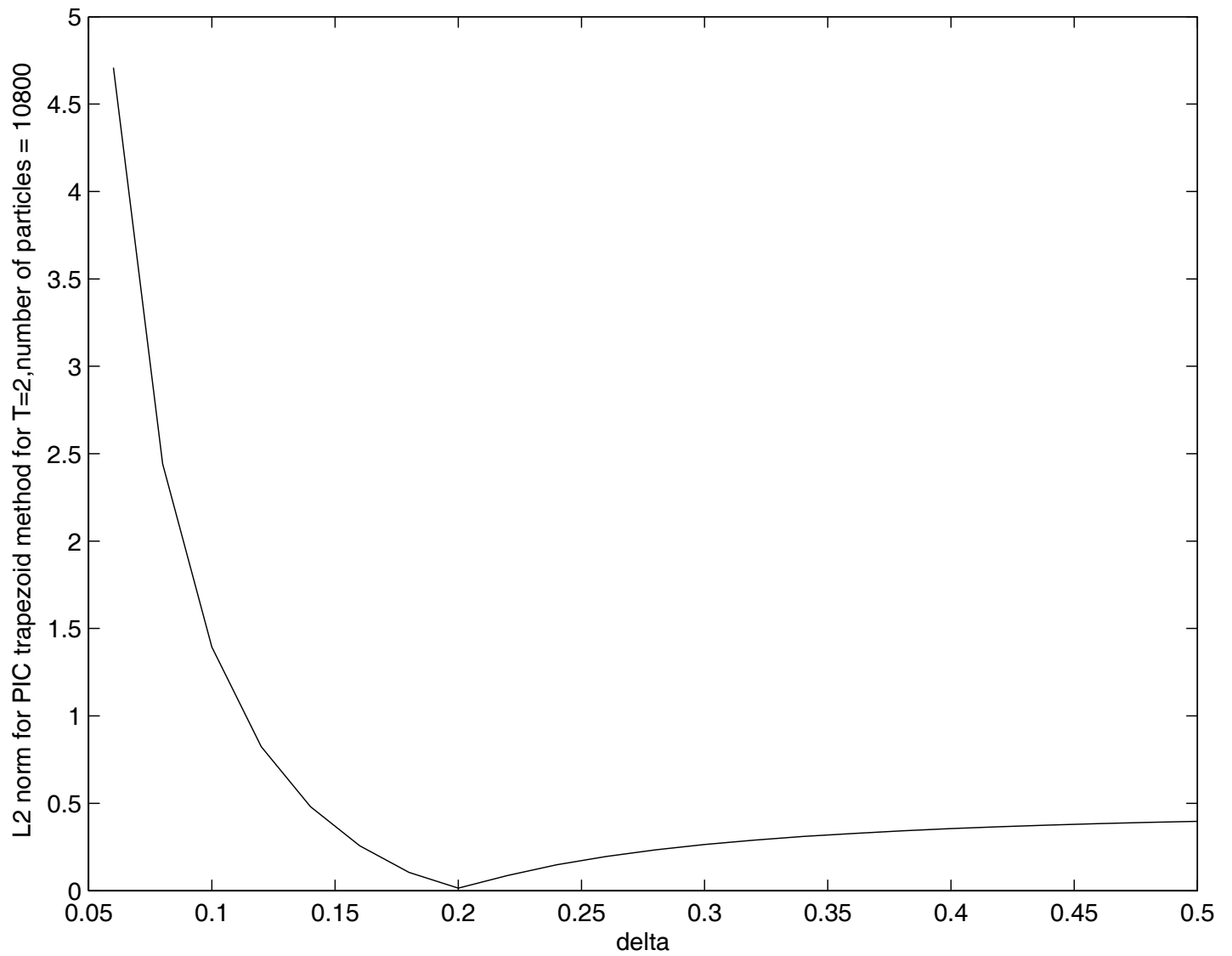


FIGURE 10. *Harmonic oscillator, trapezoid integration.*

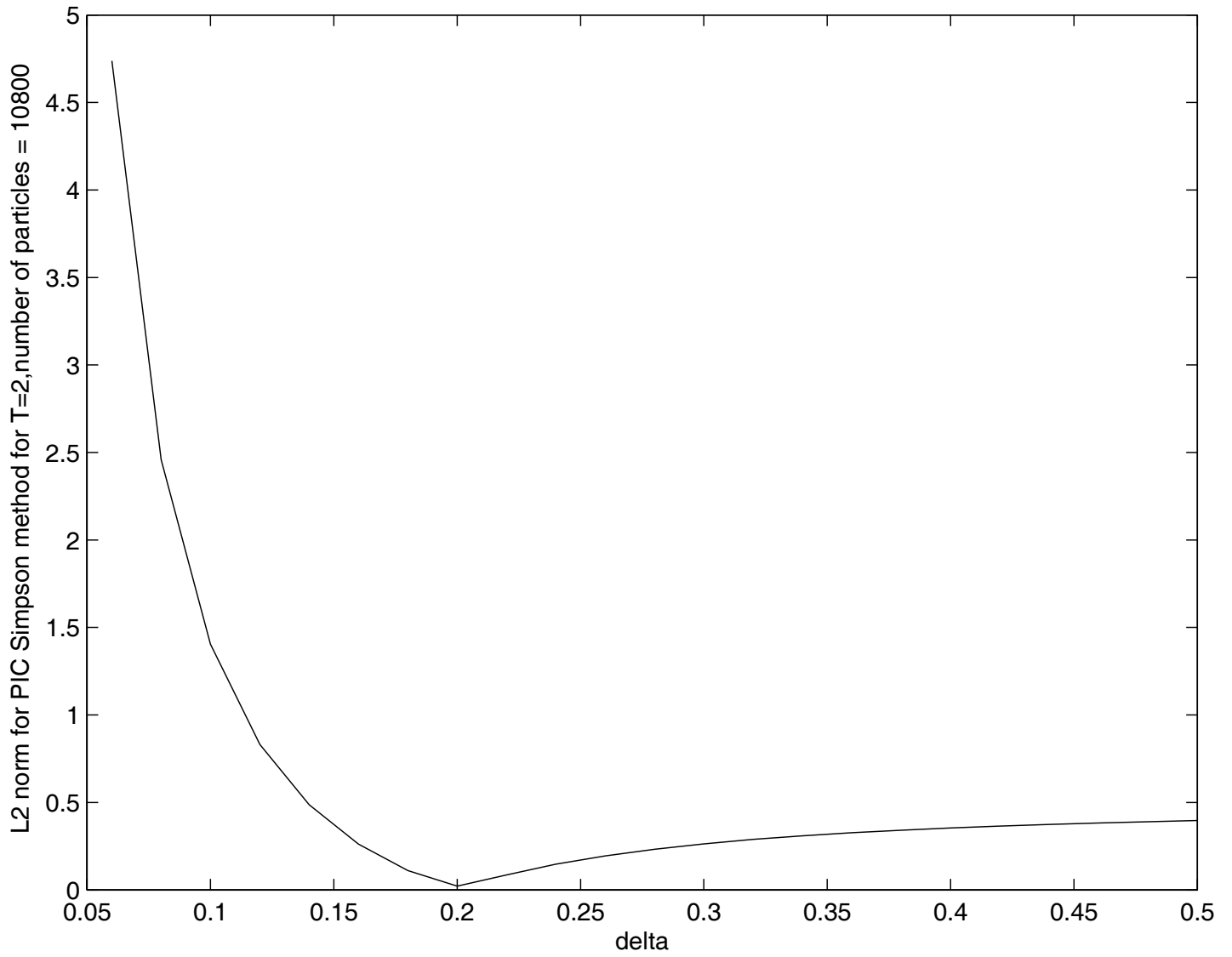


FIGURE 11. *Harmonic oscillator, Simpson integration.*

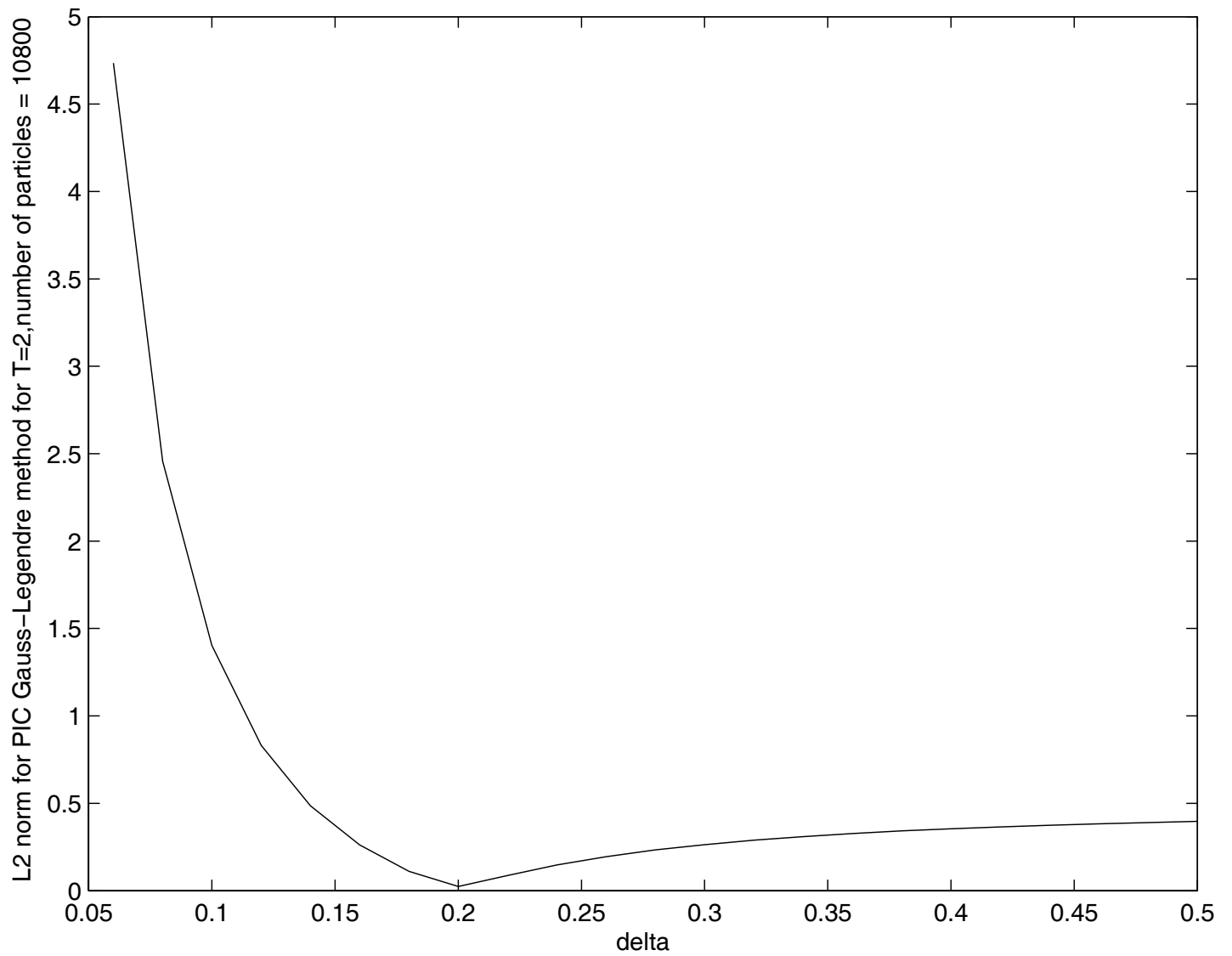
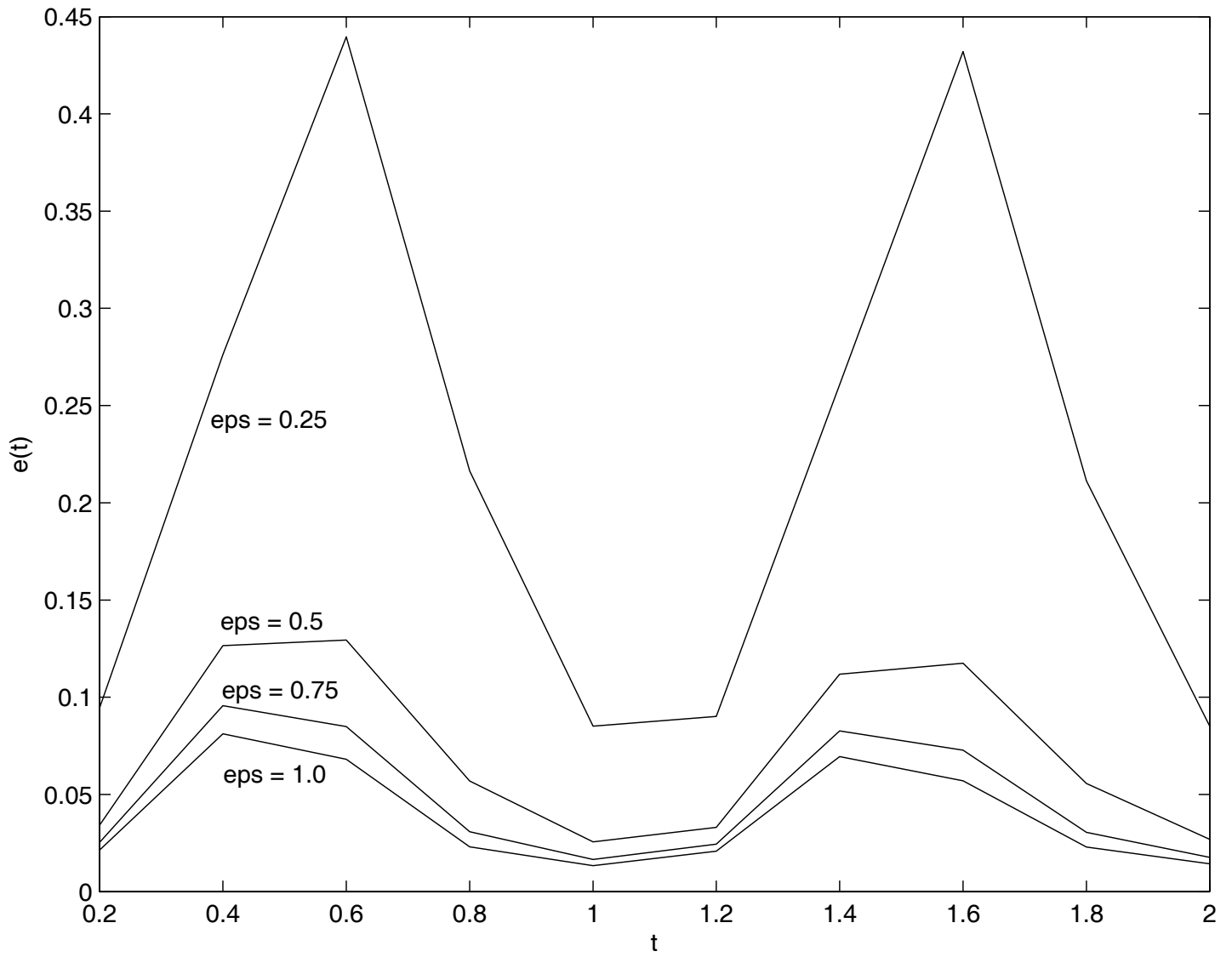
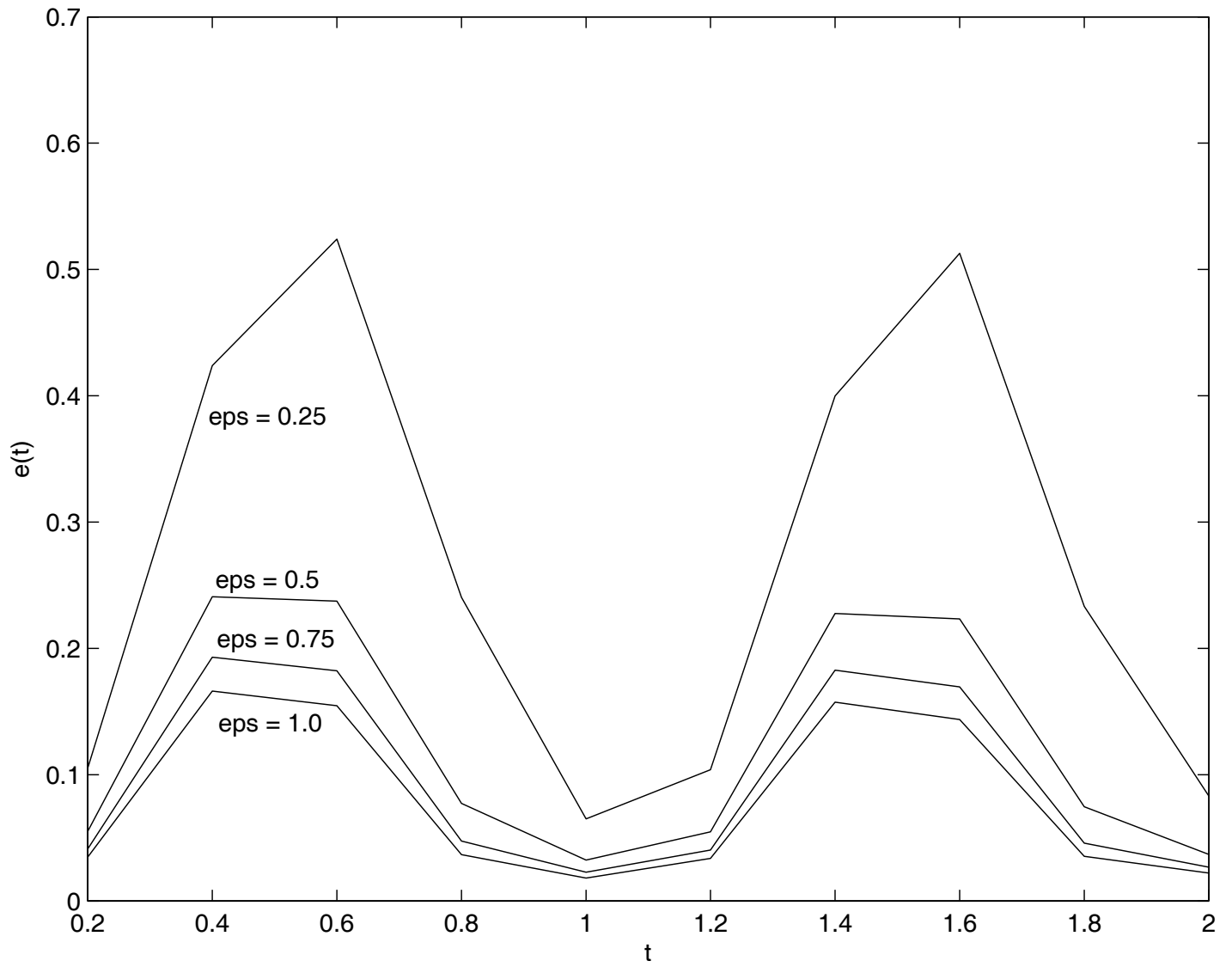


FIGURE 12. *Harmonic oscillator, Gauss – Legendre integration.*

FIGURE 13. *Harmonic oscillator, trapezoid integration.*

FIGURE 14. *Harmonic oscillator, Simpson integration.*

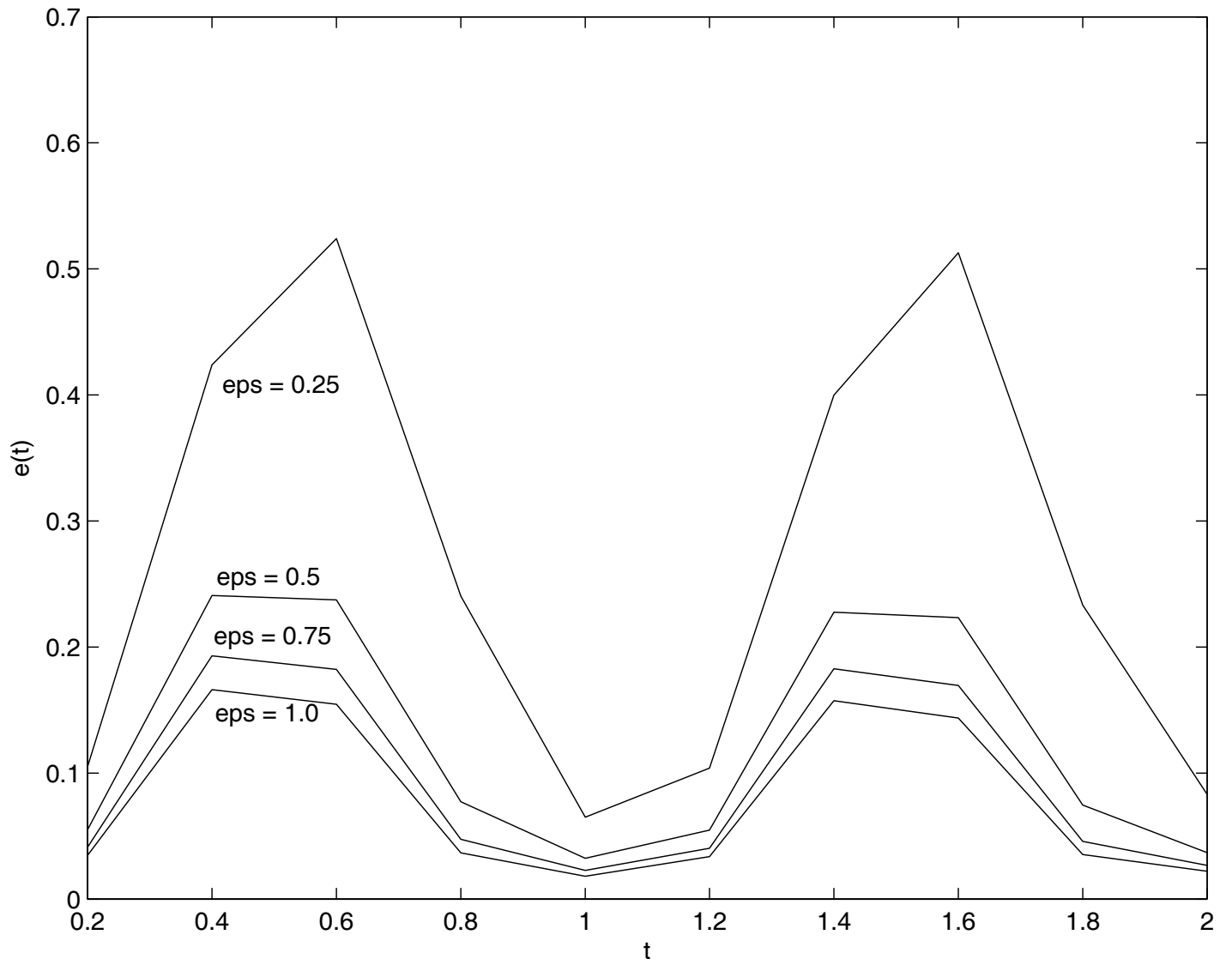
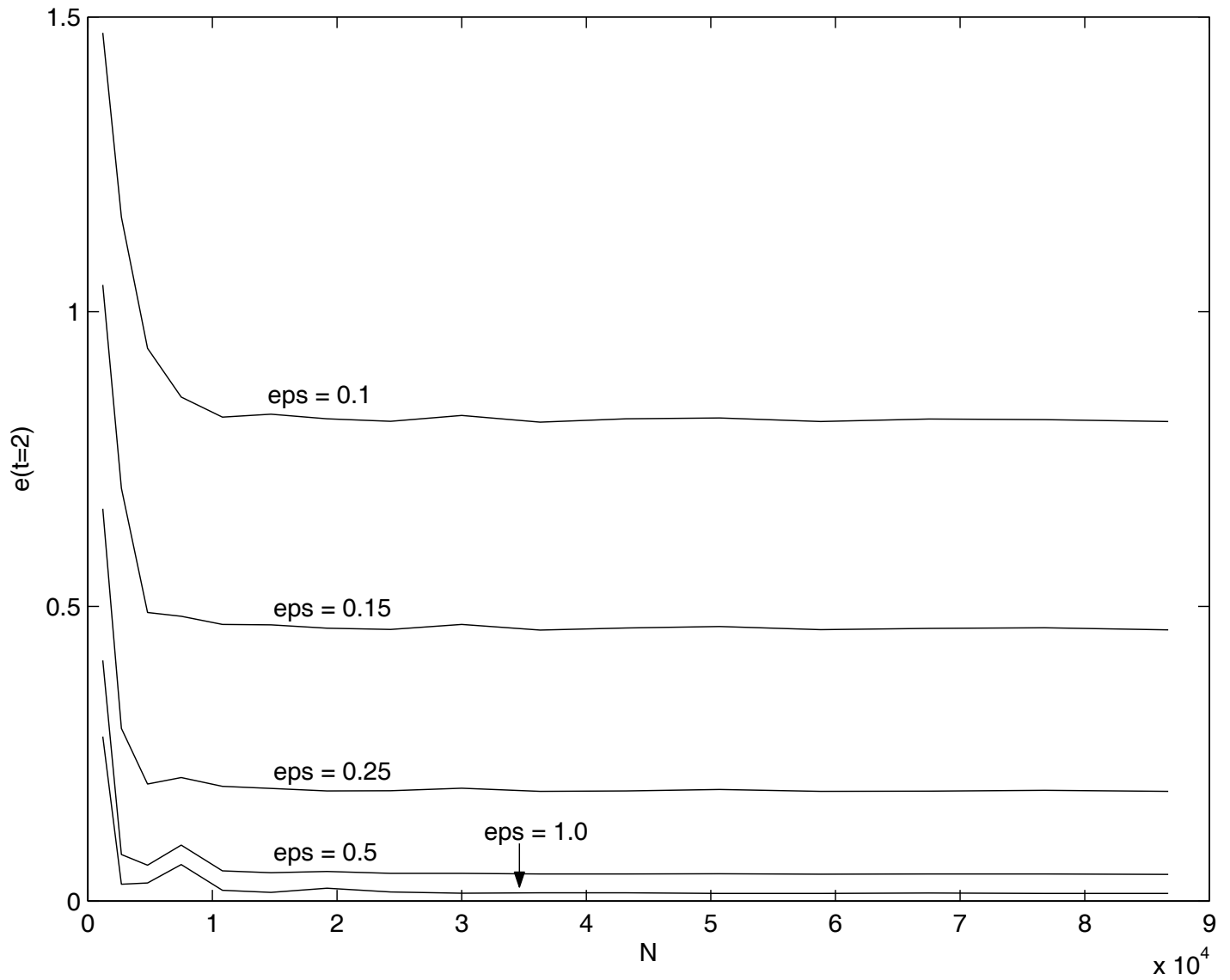
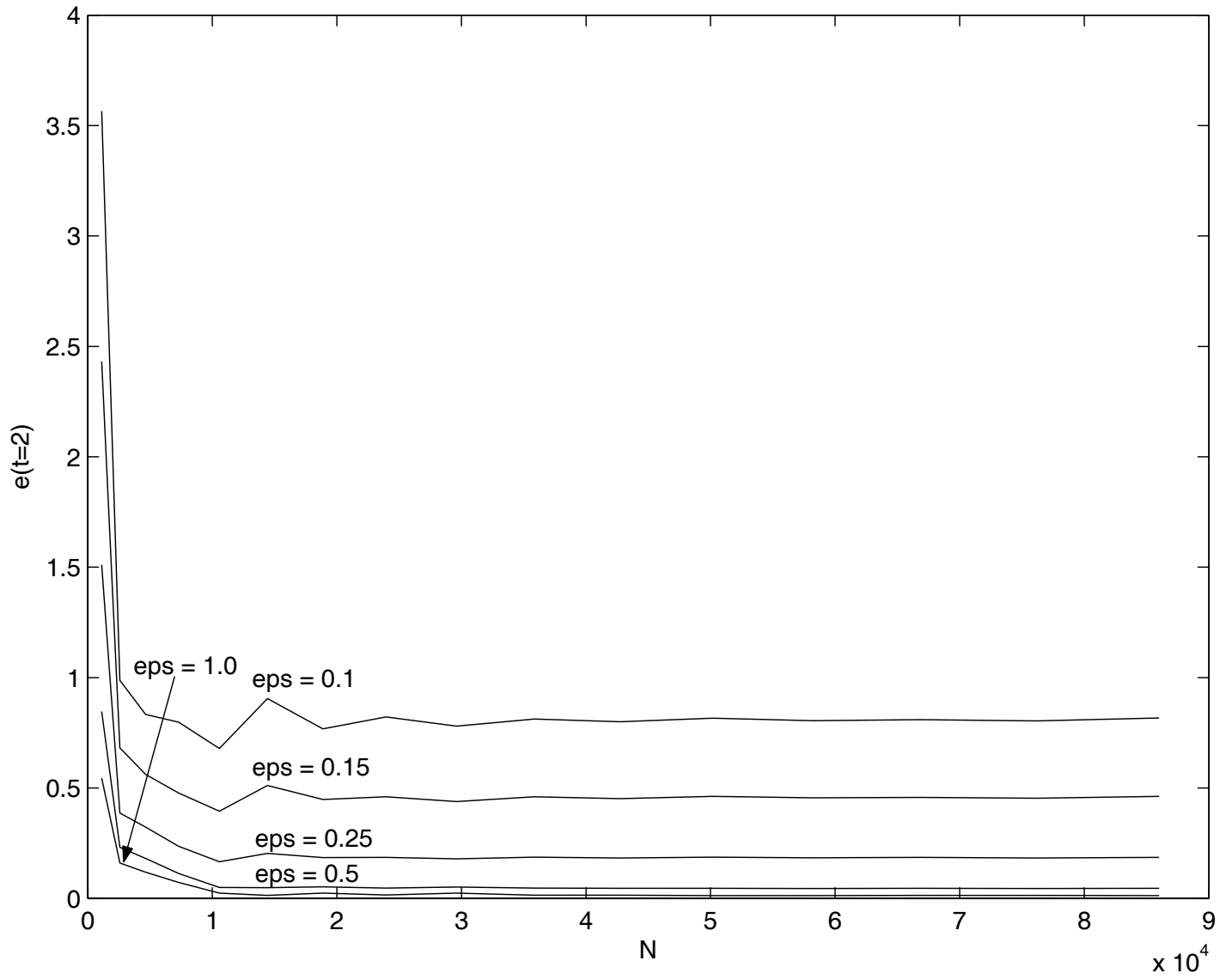
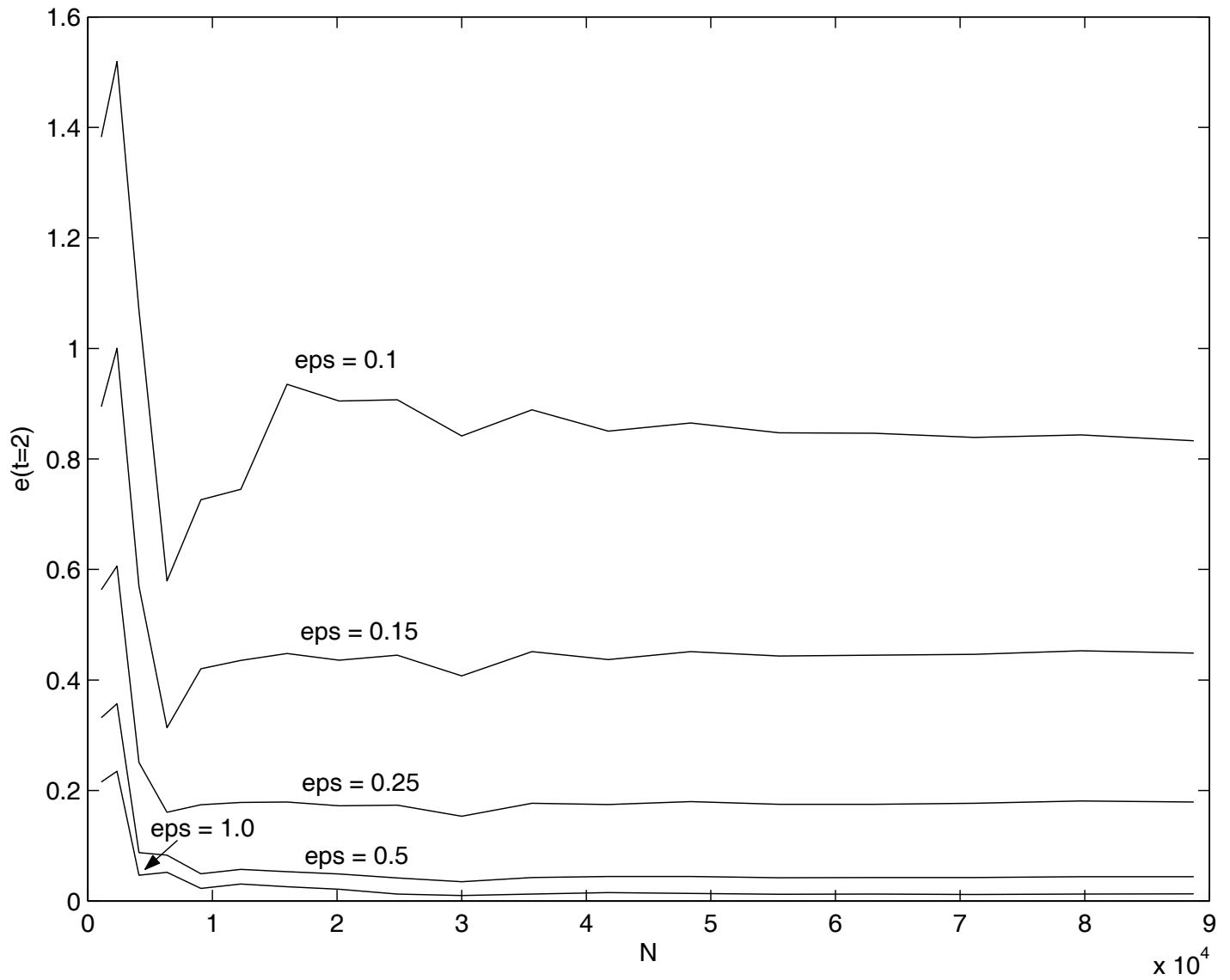


FIGURE 15. *Harmonic oscillator, Gauss – Legendre integration.*

FIGURE 16. *Harmonic oscillator, trapezoid integration.*

FIGURE 17. *Harmonic oscillator, Simpson integration.*

FIGURE 18. *Harmonic oscillator, Gauss – Legendre integration.*

QUARTIC OSCILLATOR.**VARIATION OF THE AMPLITUDE $A = |\psi^\epsilon|$ vs. x** **COMPARISON BETWEEN PIC/TRAPEZOID INTEGRATION (asterisks)****and FEM (continuous line) SOLUTIONS****N=57000 (Figs. 20-23), N=3600 (Figs. 24-26) and N=10000 (Figs. 27-29)**

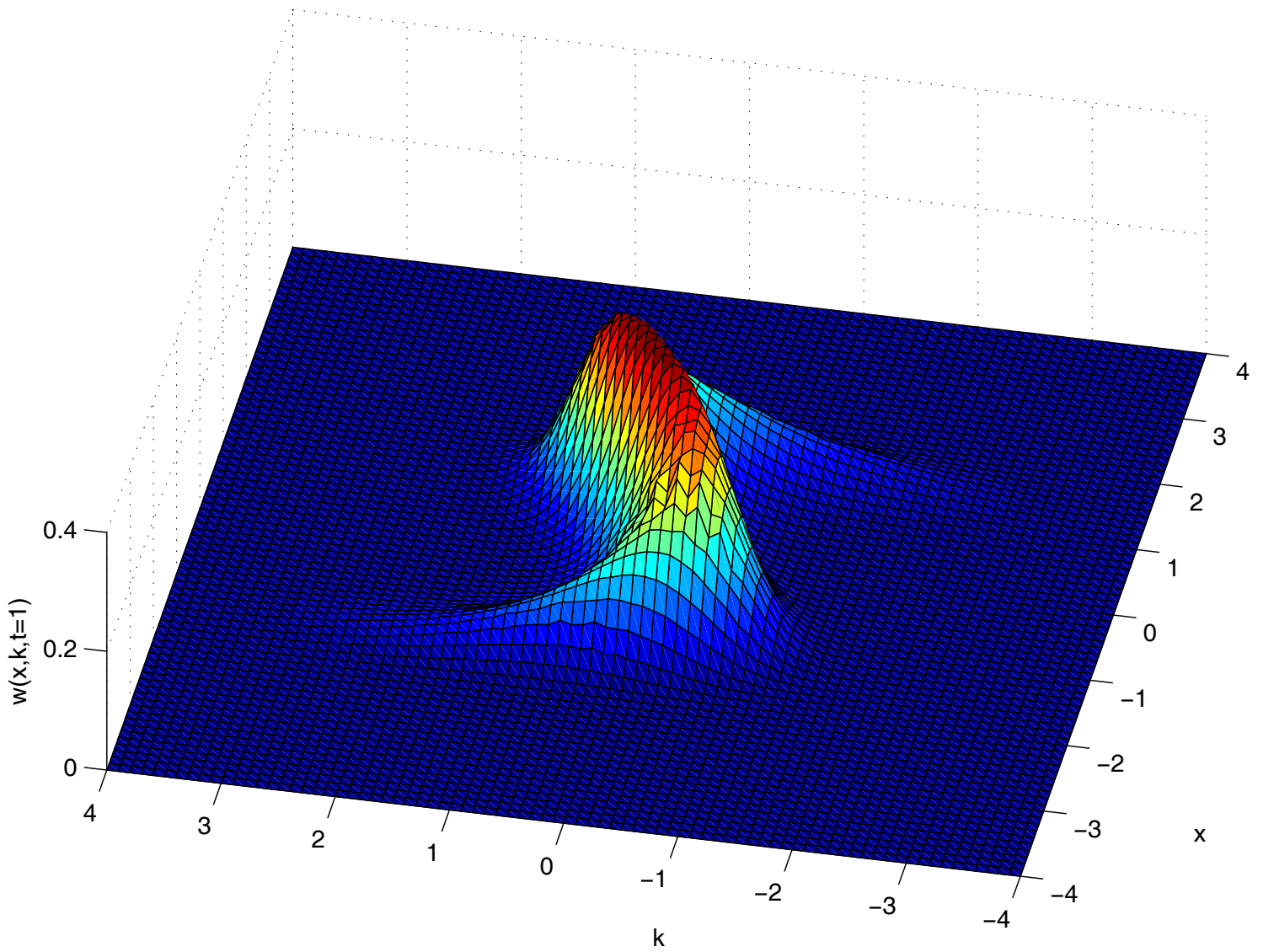


FIGURE 19. *Quartic oscillator* ($\epsilon = 1.0$, $t = 0.6$, $N = 57000$).

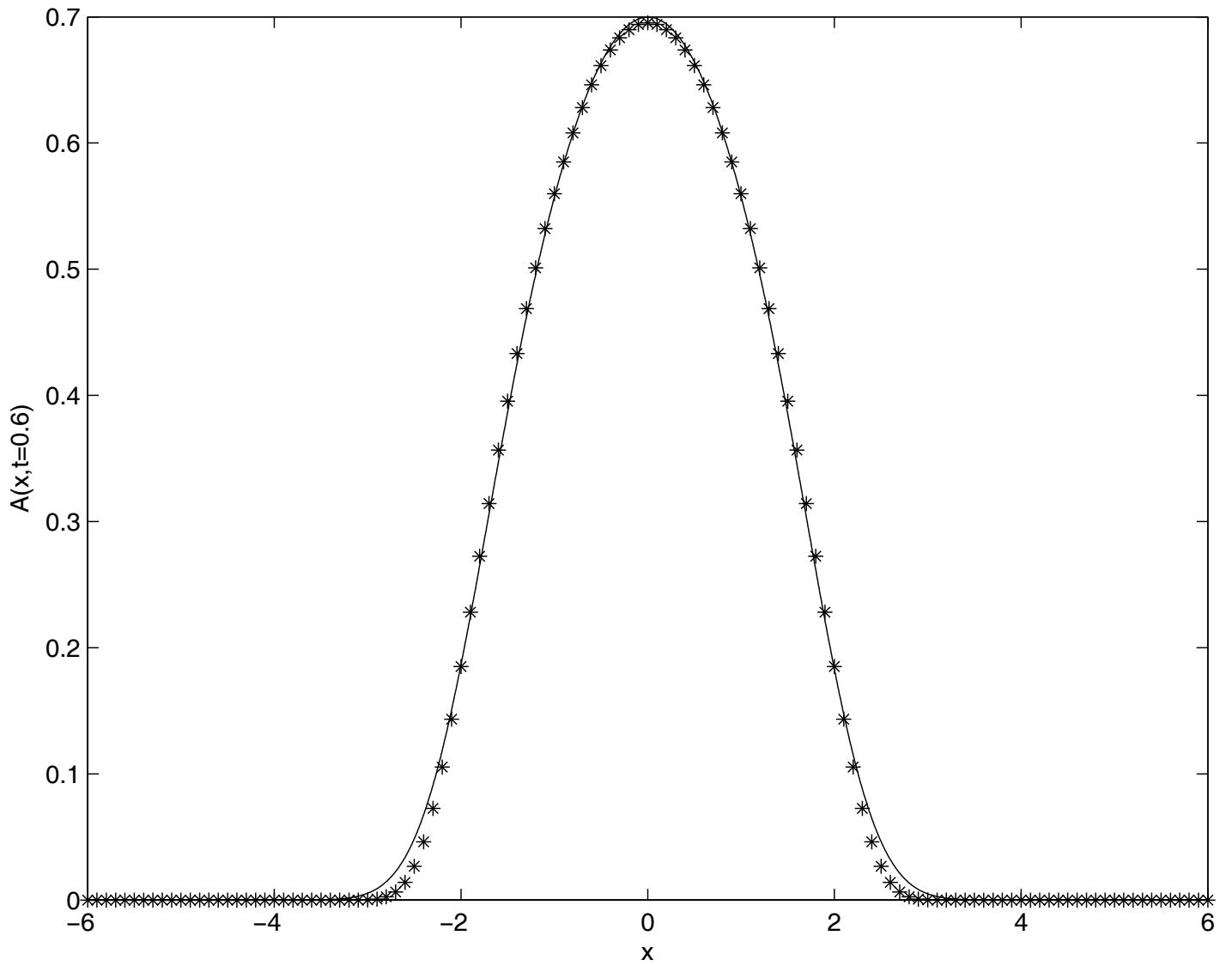


FIGURE 20. *Quartic oscillator* ($\epsilon = 1.0$, $t = 0.6$, $N = 57000$).

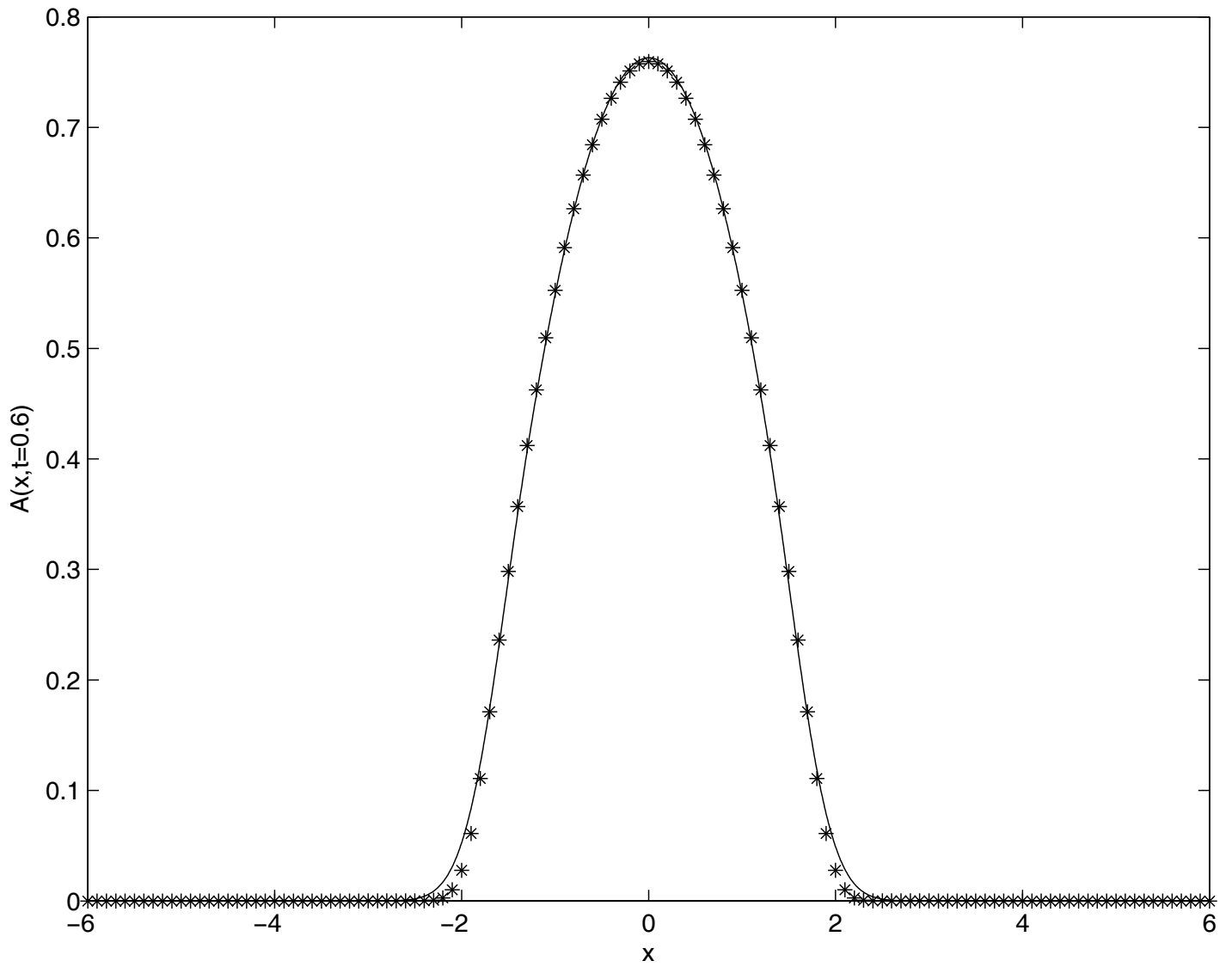


FIGURE 21. *Quartic oscillator* ($\epsilon = 0.5$, $t = 0.6$, $N = 57000$).

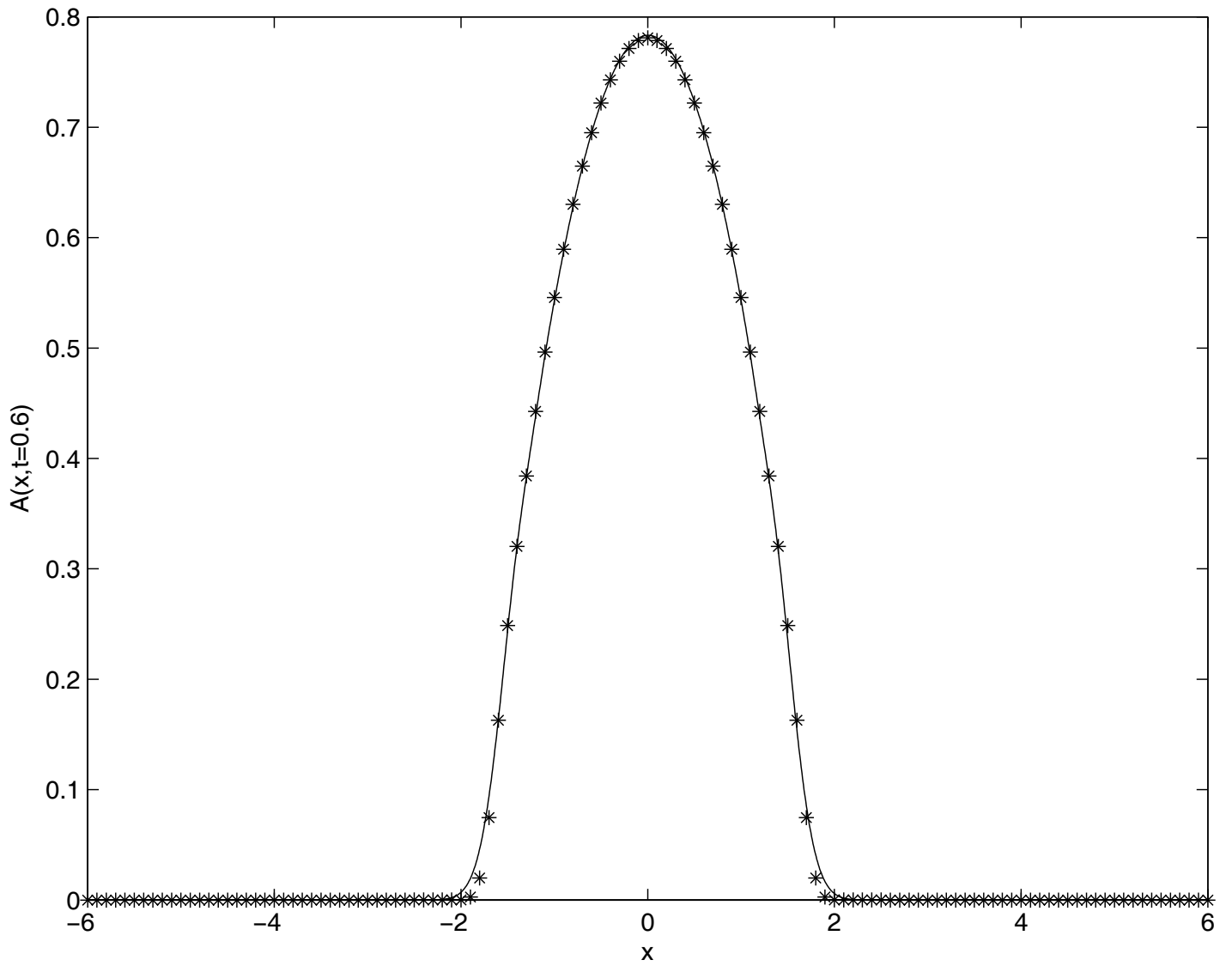
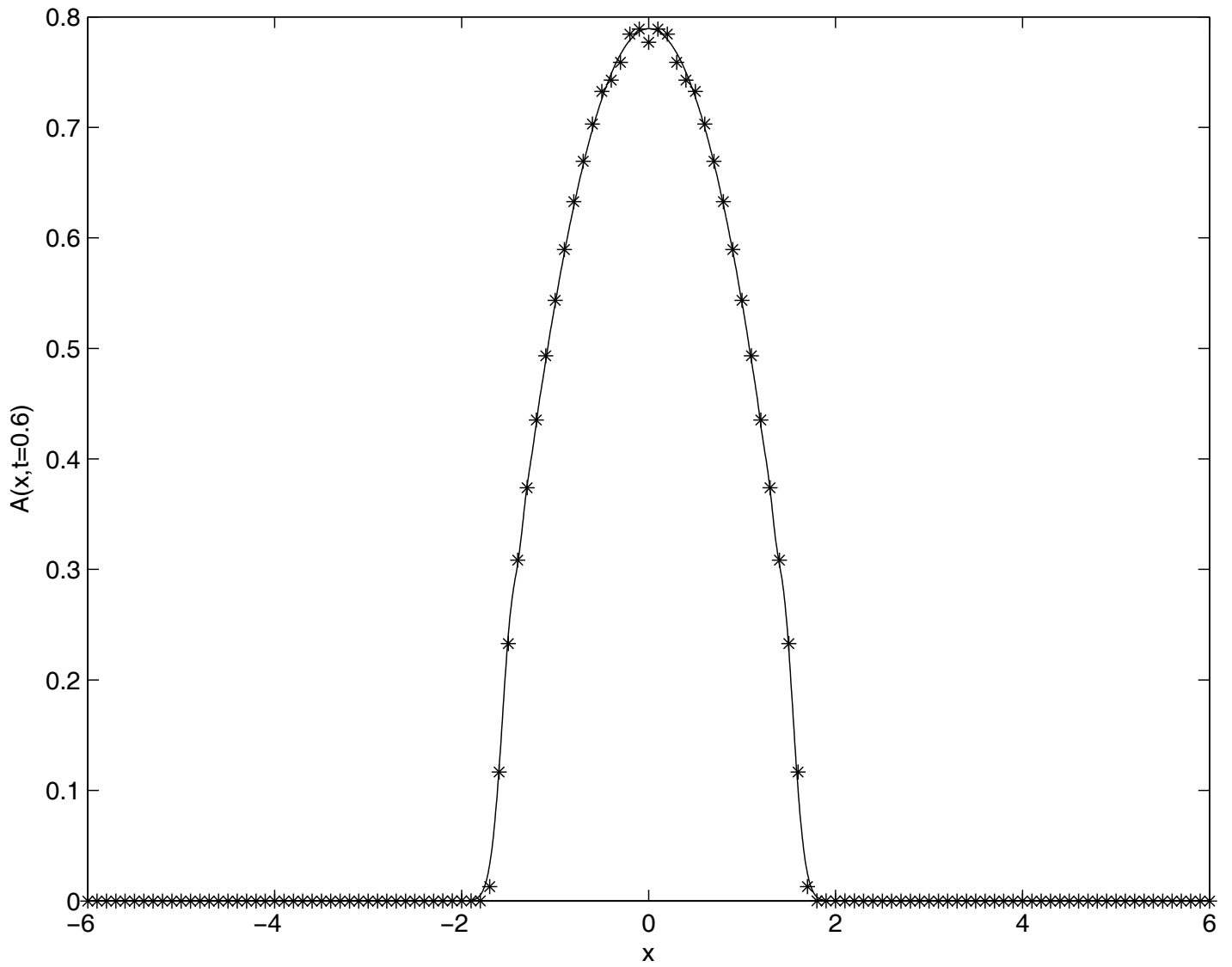


FIGURE 22. *Quartic oscillator* ($\epsilon = 0.25$, $t = 0.6$, $N = 57000$).

FIGURE 23. *Quartic oscillator* ($\epsilon = 0.10$, $t = 0.6$, $N = 57000$).

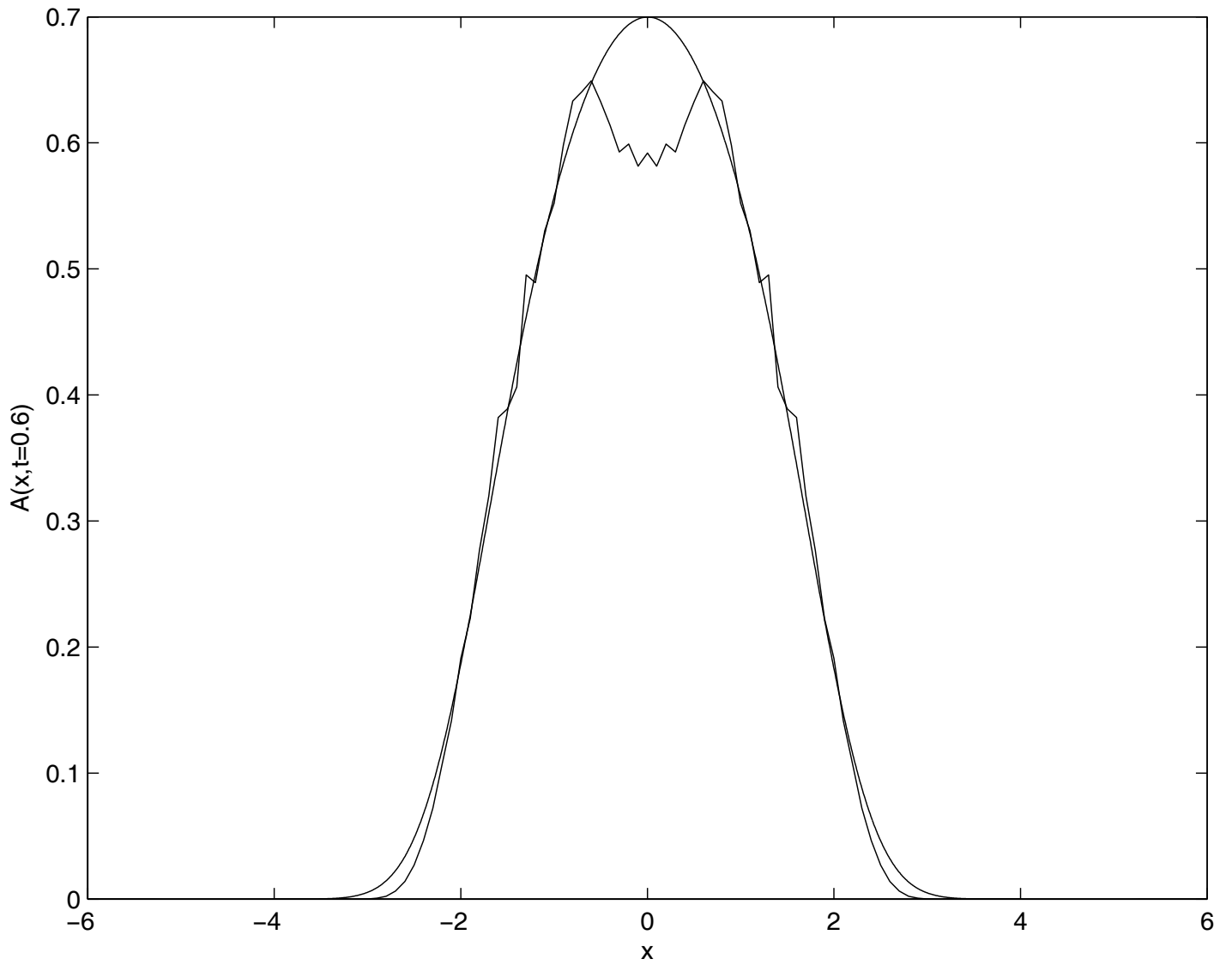


FIGURE 24. *Quartic oscillator* ($\epsilon = 1.0$, $t = 0.6$, $N = 3600$).

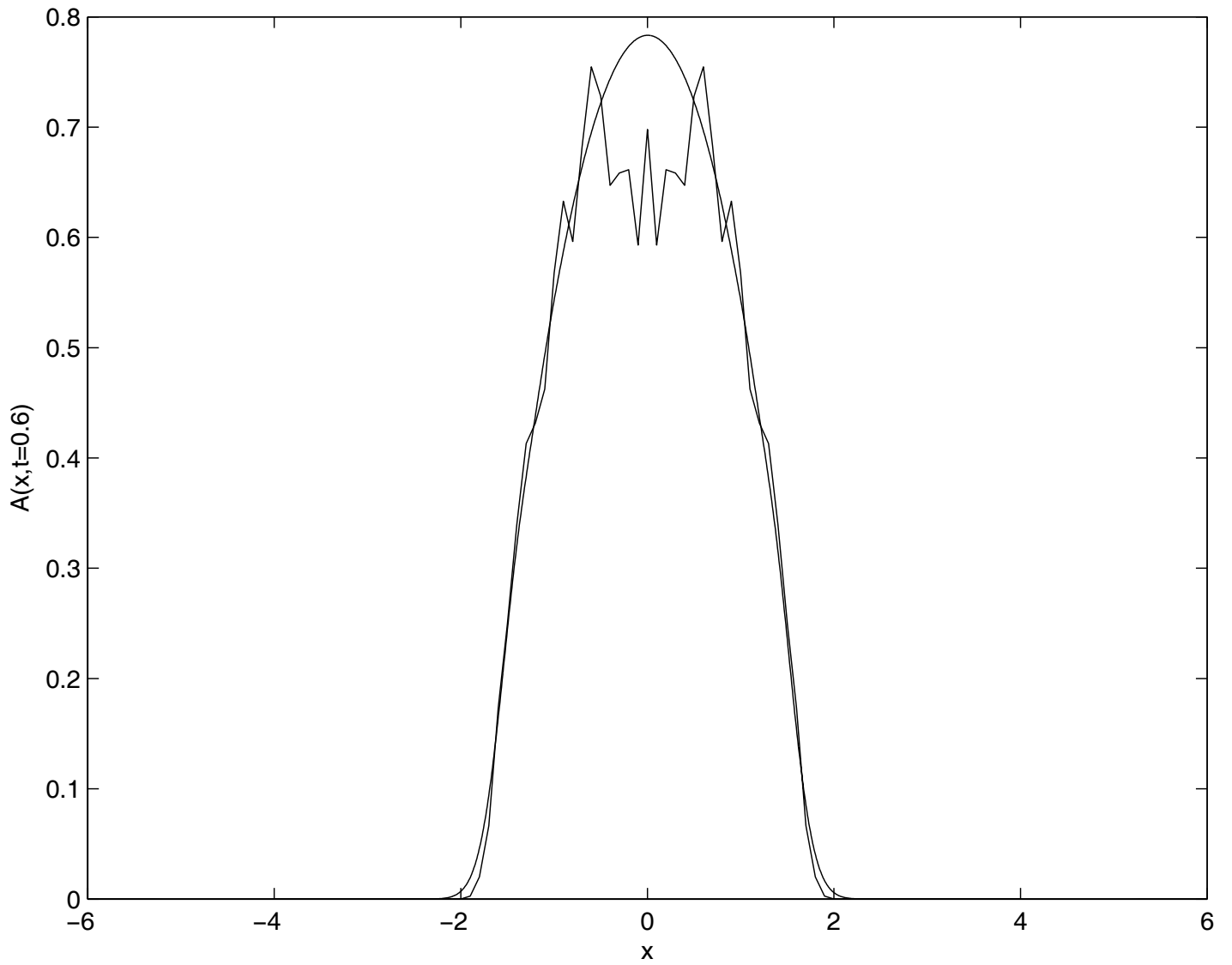


FIGURE 25. *Quartic oscillator* ($\epsilon = 0.25$, $t = 0.6$, $N = 3600$).

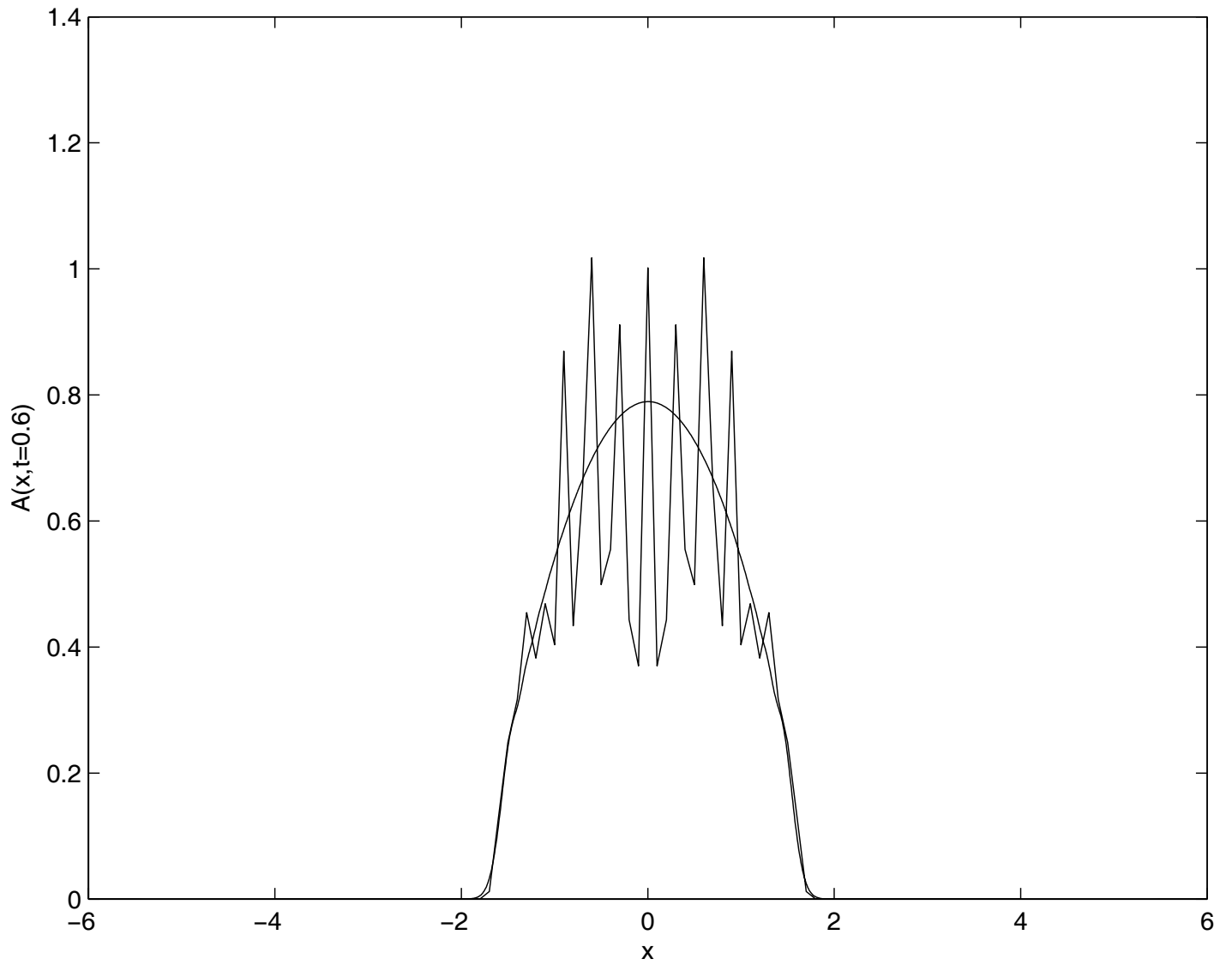


FIGURE 26. *Quartic oscillator* ($\epsilon = 0.10$, $t = 0.6$, $N = 3600$).

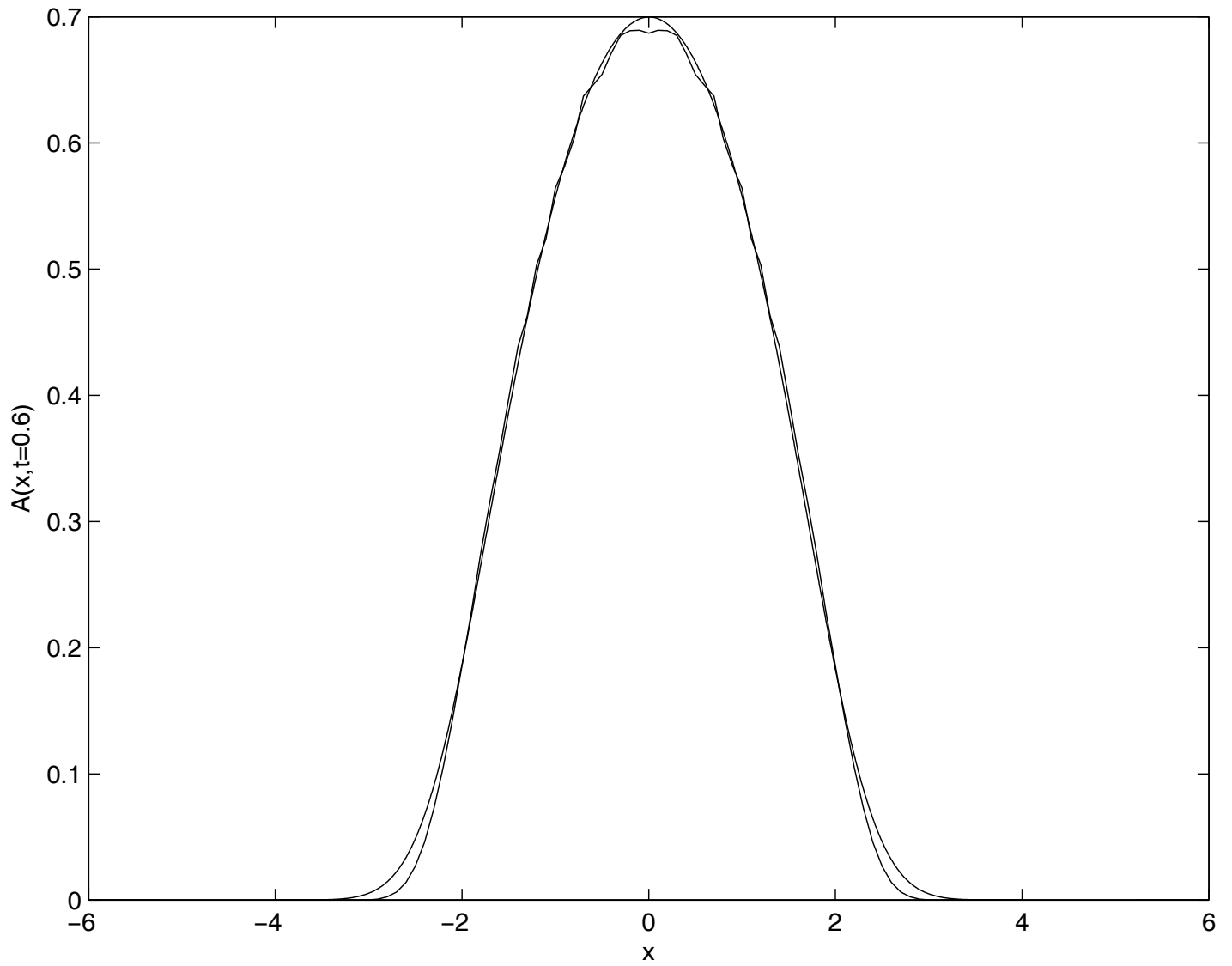


FIGURE 27. *Quartic oscillator* ($\epsilon = 1.0$, $t = 0.6$, $N = 10000$).

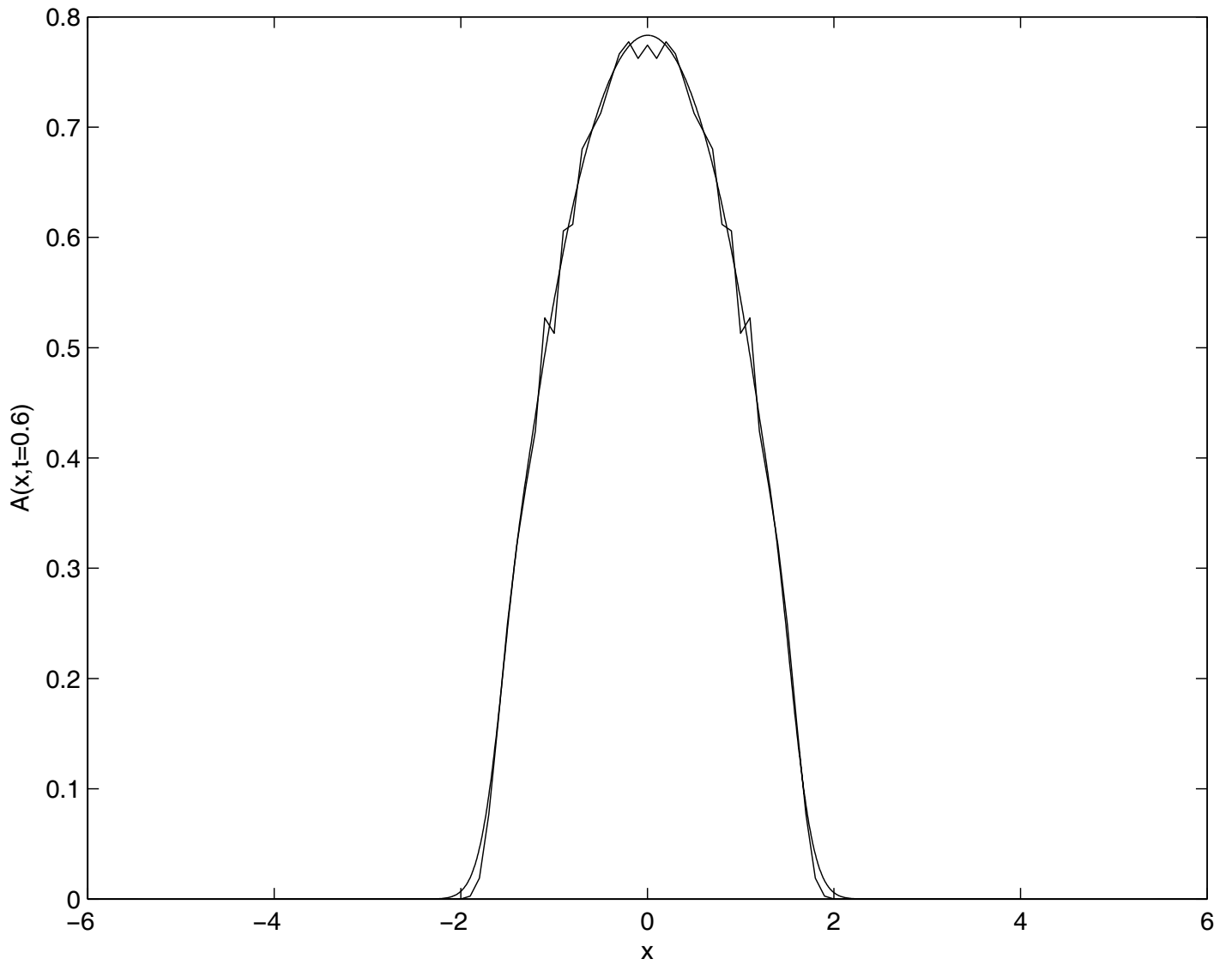


FIGURE 28. *Quartic oscillator* ($\epsilon = 0.25$, $t = 0.6$, $N = 10000$).

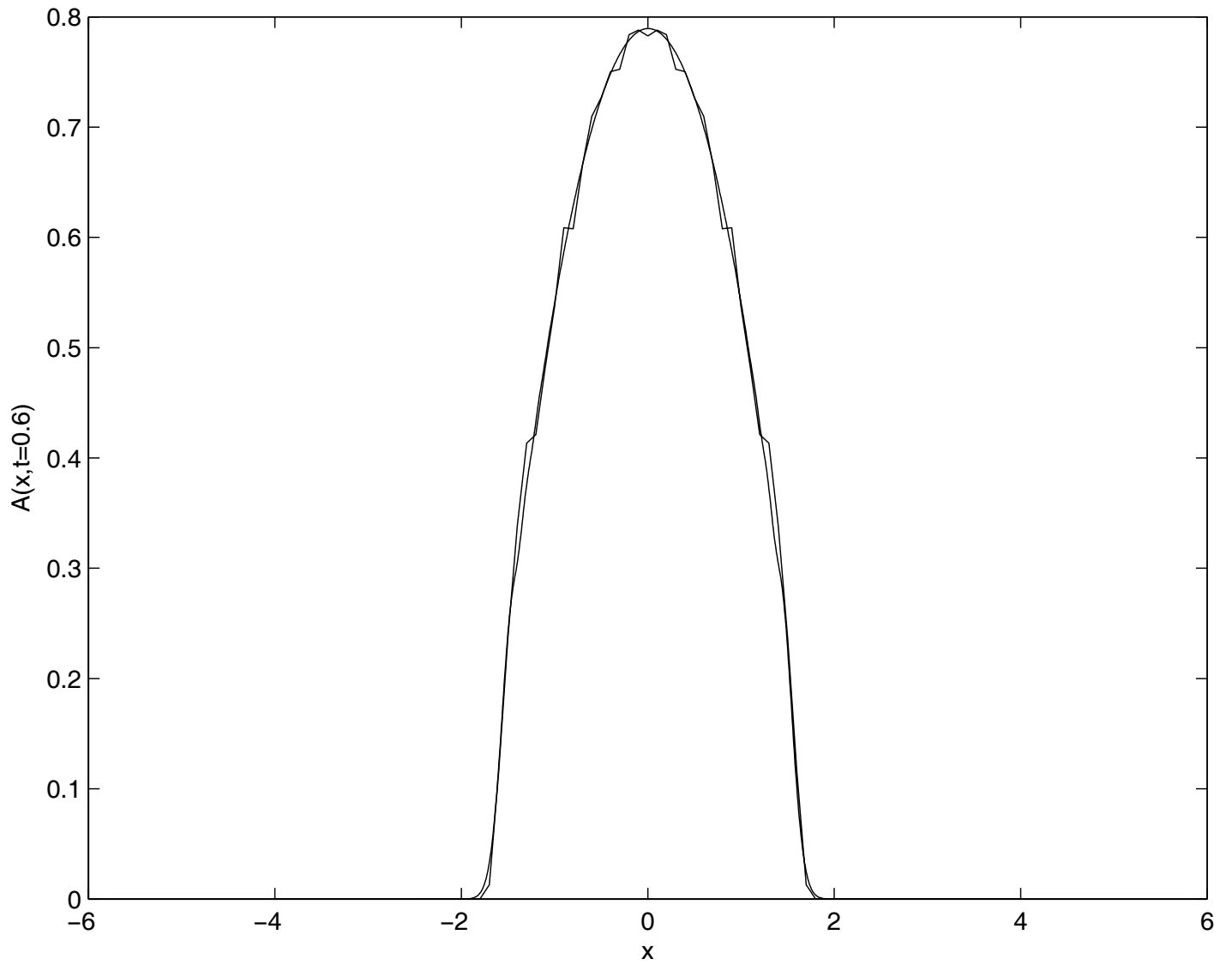


FIGURE 29. *Quartic oscillator* ($\epsilon = 0.10$, $t = 0.6$, $N = 10000$).

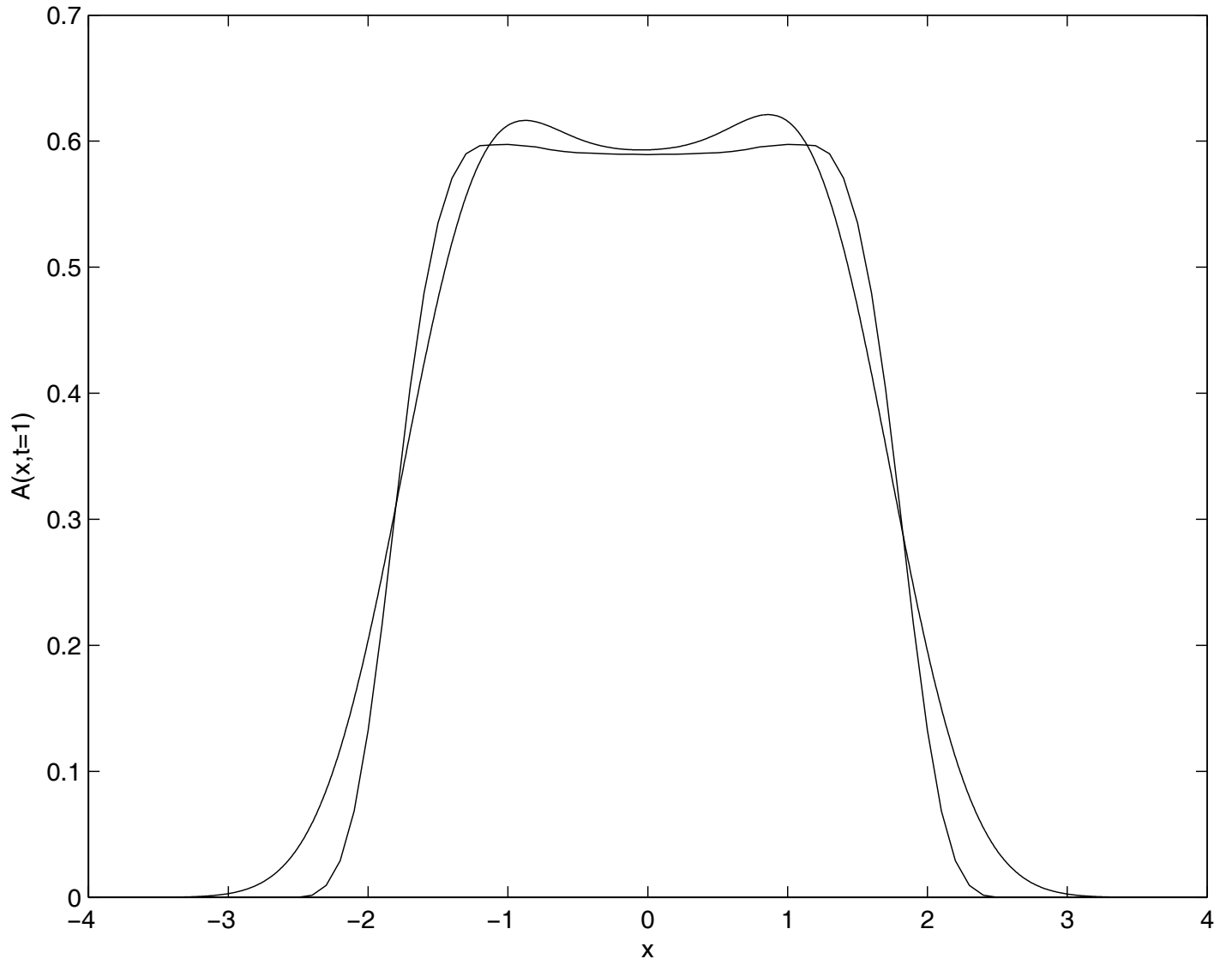


FIGURE 30. *Quartic oscillator* ($\epsilon = 1.0$, $t = 1.0$, $N = 57000$).

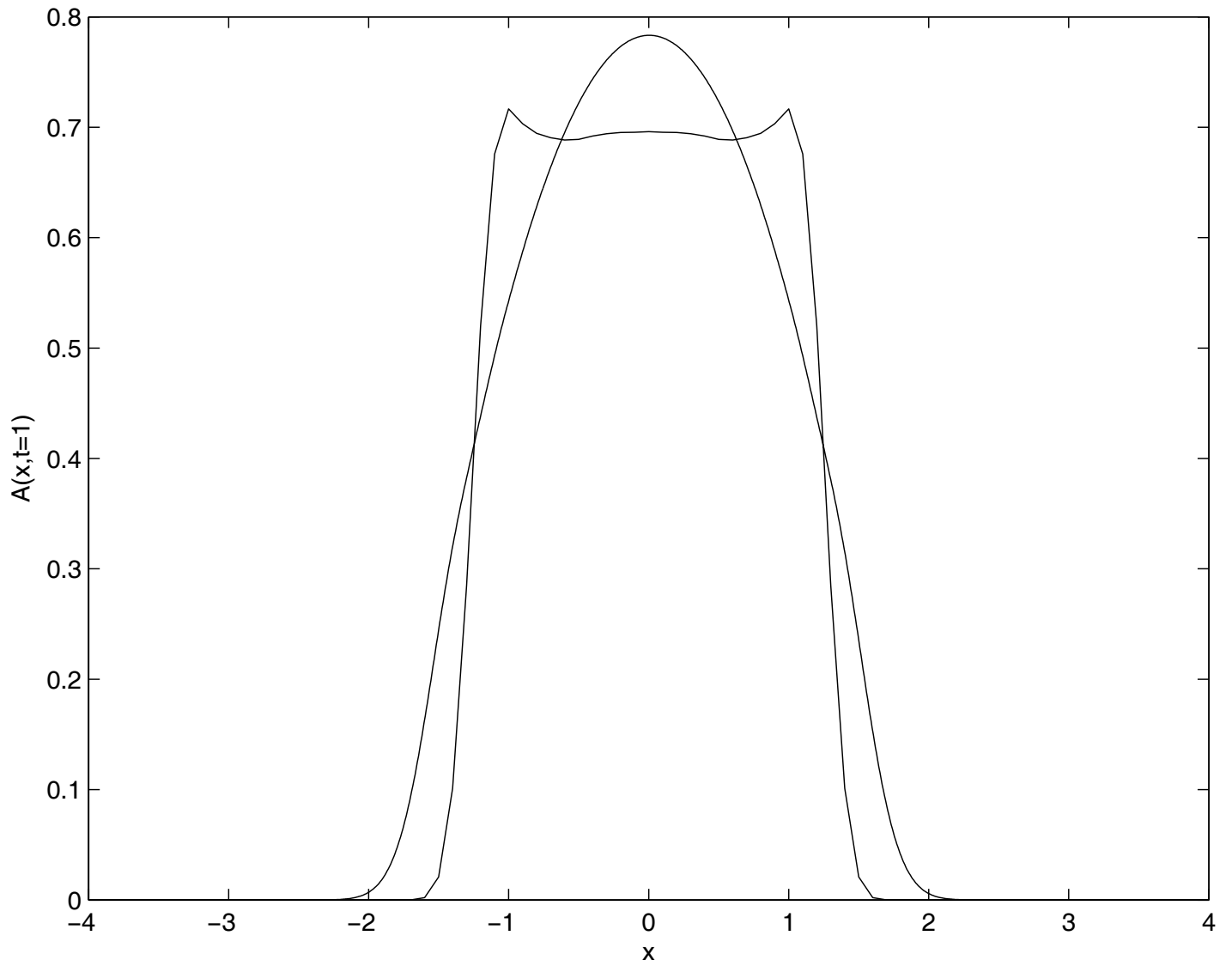


FIGURE 31. *Quartic oscillator* ($\epsilon = 0.25$, $t = 1.0$, $N = 57000$).

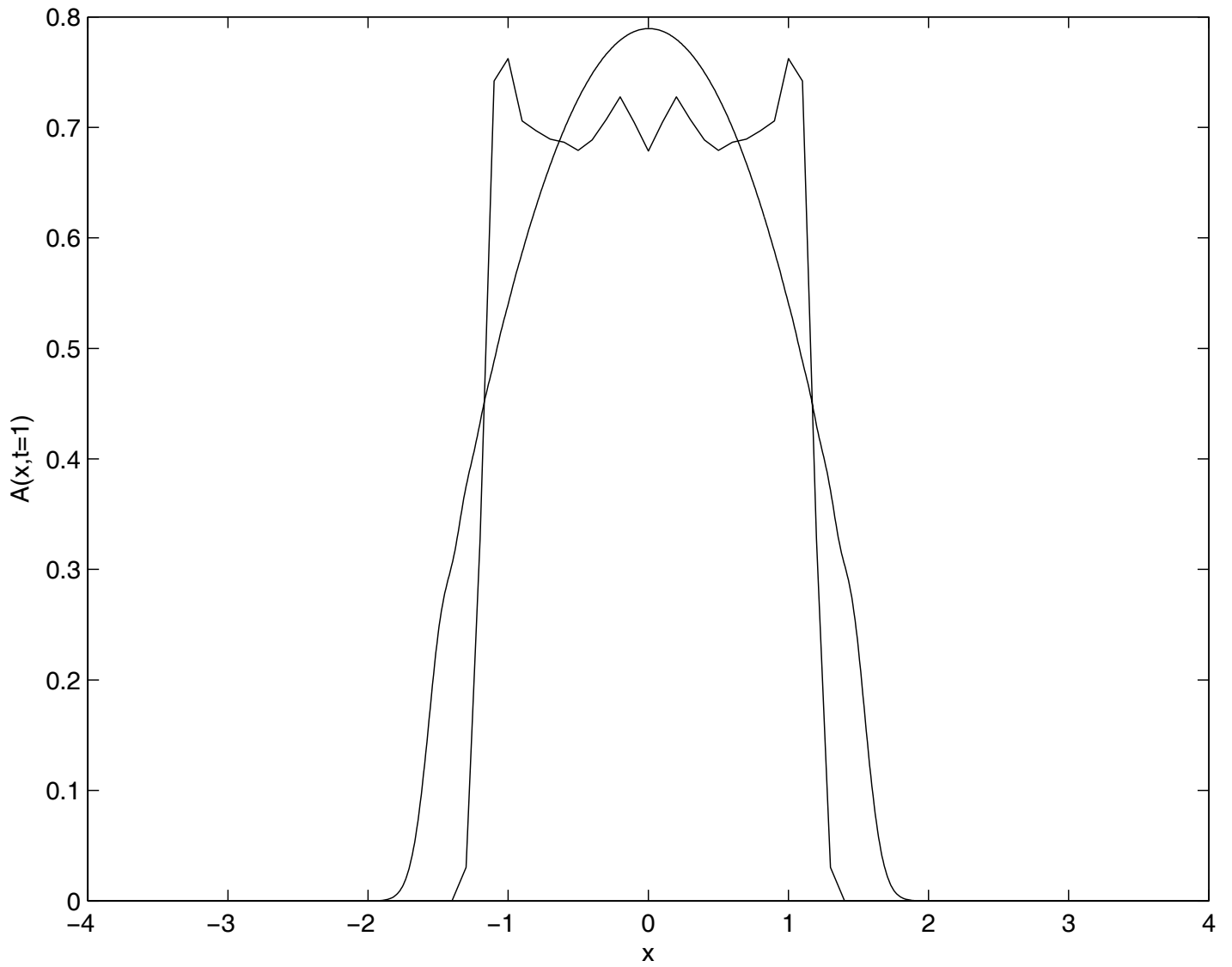


FIGURE 32. *Quartic oscillator* ($\epsilon = 0.10$, $t = 1.0$, $N = 57000$).